R. & M. No. 2690
(10,685, 11,410)
A.R.C. Technical Report

MINISTRY OF SUPPLY

AERONAUTICAL RESEARCH COUNCIL
REPORTS AND MEMORANDA

The Royal Aircraft Establishment 4 ft × 3 ft Experimental Low Turbulence Wind Tunnel

PART I.—General Flow Characteristics

By

H. B. SQUIRE, M.A. and K. G. WINTER, B.Sc.

LONDON: HER MAJESTY'S STATIONERY OFFICE

1953

PRICE 7s 6d NET

The Royal Aircraft Establishment 4 ft × 3 ft Experimental Low Turbulence Wind Tunnel

PART I.—General Flow Characteristics

By

H. B. SQUIRE, M.A. and K. G. WINTER, B.Sc.

COMMUNICATED BY THE PRINCIPAL DIRECTOR OF SCIENTIFIC RESEARCH (AIR), MINISTRY OF SUPPLY

Reports and Memoranda No. 2690*

February, 1948

Summary.—The 4 × 3 ft Wind Tunnel was erected as a model of larger tunnels to investigate unconventional design features directed towards obtaining a high standard of flow. Diffusers of 5 deg cone angle are used, except for the rapid expansion through three wire-gauze screens up to the maximum section. The contraction ratio is 31·2 : 1 and nine screens are fitted in the maximum section. A speed control is used operating independently of the fan by means of a by-pass duct.

The velocity distribution across the working-section is constant to $\pm \frac{1}{4}$ per cent. The standard deviation of the velocity with time measured over a period of 50 sec is 0·03 per cent.

The flow in the diffusers shows no tendency to separate and the velocity distribution approaching the first screen is very satisfactory.

The installation of cascades with gap/chord ratio of $\frac{1}{4}$ gives uniform outlet flow without appreciable increase in the pressure drop.

There is no separation in the rapid expansion of the bulge, but the flow in the contraction cone is not satisfactory. A longer contraction would have been advantageous.

The power factor has been measured as 0·27 with all screens fitted but could be improved slightly if all the leaks were sealed.

The speed control is satisfactory in operation.

1. *Introduction.*—During the past few years it has become evident that the standard of flow achieved in wind tunnels of conventional design falls short of that required to give useful results on any problem where boundary-layer transition is of importance, and that the unsteady flow is a source of unnecessary inconvenience in the taking of readings. Experience[1] in the Royal Aircraft Establishment, No. 2, $11\frac{1}{2} \times 8\frac{1}{2}$ ft Wind Tunnel has shown that a reasonably good standard of flow can be obtained in a conventional type of tunnel, but only at the cost of many detailed changes involving much time in installation and considerable power in operation. The obvious changes to make in future design work were firstly to reduce the rate of expansion in the diffusers, and secondly to increase the contraction ratio. These changes would lead to a tunnel of great circuit length and it was thought that a rapid expansion should be incorporated at some stage.

* R.A.E. Report Aero. 2182, received 26th June, 1947. R.A.E. Report Aero. 1937, received 15th April, 1948.

In view of the proposal, under the Bedford scheme, to erect several new tunnels, it was decided that a model tunnel, using these unconventional design features, should be erected. It was found that a tunnel of working-section 4 × 3 ft (Ref. 2) could be housed in the building then occupied by the R.A.E. No. 1, 7-ft Wind Tunnel. The construction was started in November, 1944, and finished in March, 1946.

This report describes the general characteristics of the tunnel and its flow. The results of measurements of turbulence will be issued subsequently.

2. *Description of the Tunnel.*—2.1. *General Description.*—The tunnel is of the single return-circuit type with closed working-section, the fan being installed downstream of the second corner (Fig. 1). The four corners are fitted with conventional cascades. The cross-section is that of a regular octagon apart from the working-section, first diffuser and fan section. The working-section is enclosed by the observation chamber which can be sealed. No provision is made for a balance. The tunnel is of wooden construction supported on a steel framework.

The unconventional features are

(a) The use of diffusers of 5 deg cone angle instead of the usual 7 deg.

(b) The method of obtaining the large contraction ratio of 31·2: 1. To keep down the length of the tunnel the last part of the expansion is made rapidly through spaced wire-gauze screens.

(c) The insertion of nine wire-gauze screens in the maximum section or ' bulge '.

(d) The method of speed control by adjusting the flow through a duct by-passing the working-section.

2.2. *Working-Section.*—The working-section is 11 ft long, of basically rectangular section 4 ft wide by 3 ft high, with fillets in the four corners. The length of side of the fillets at the middle of the working-section is 8·1 in. The fillets are tapered to allow for the increase of the boundary-layer thickness along the wall (*see* Section 4.2).

Eight vent holes, of total area roughly 2 sq ft, are provided at the downstream end of the working section.

Access to the inside of the tunnel is provided by hinging outwards the last third of both the vertical walls and of the floor. The front third of the floor can also be lowered (Fig. 2).

2.3. *First Diffuser.*—From the working-section there is an expansion of area ratio 2·44: 1 up to the first corner. The rate of expansion is equivalent to that of a circular cone of total angle 5·2 deg. During the expansion the section changes from octagonal to circular. A wire safety net is installed near the end of the diffuser.

2.4. *First and Second Corners.*—At both the first and second corners there are fourteen turning vanes of chord 26 in. and spacing $6\frac{1}{2}$ in. (Fig. 3). The trailing edge of each vane is in the form of an adjustable flap of 6-in. chord. The flaps are made in three independently adjustable portions as shown in Fig. 6, and are held in position by rods attached to the adjacent vanes.

In order to eliminate pressure gradients at the junctions of the walls and vanes the wall shape, in the passage between any two vanes, is modified to approximate to that of the surface of a cone, the axis of which coincides with that of the concave face of the passage.

The section is circular and of constant area between the two corners.

2.5. *Fan Installation* (Fig. 4).—Constant cross-sectional area is maintained up to the fan by expanding the tunnel walls round the fan boss. Five pre-rotation vanes upstream of the fan, and seven straighteners downstream support the sheet metal fan boss fairing.

The fan was designed to fit an existing electric motor which provides 200 h.p. at 650 r.p.m. giving a tip speed of 245 ft/sec for an 86-in. diameter fan. A high-solidity fan was required to transmit the power to the wind stream, and this in turn led to a large boss diameter of 4 ft to avoid a solidity greater than unity at the inner end of the fan blades. Apart from these features the fan is conventional with six blades each of constant chord 26 in., and constant thickness 12·7 per cent. The tip clearance is 0·2 in., and there are three safety trip-switches fitted in the tunnel walls round the fan.

The motor is of direct-current (D.C.) type controlled by a ' negative boost ' system and is mounted outside the tunnel on a reinforced concrete pedestal. The fan is overhung on the end of the driving shaft which is supported by three bearings, one carried by the pre-rotation vanes, one at the second corner and a thrust bearing outside the tunnel. The shaft and bearing at the second corner are enclosed by fairings (Fig. 5). Seals are provided where the shaft passes through the tunnel wall and where it enters the fan boss fairing.

2.6. *Second Diffuser.*—The expansion starts immediately downstream of the straightener vanes, the first 5 ft of the expansion being in the form of an annulus round the tail of the fan boss fairing. A change of shape from circular to octagonal is produced in this length. The remainder of the expansion is octagonal in section with straight taper. The rate of expansion is equivalent to that of a circular cone of total angle 5·2 deg. The final area is 8·5 times that of the working-section.

2.7. *Third and Fourth Corners.*—The third and fourth corners are each fitted with 24 turning vanes of chord 30 in. (including 6 in. adjustable flap at the trailing edge) and spacing 7·7 in. (Figs. 3, 6). The section is octagonal and of constant area between the two corners.

The sloping walls between the vanes are faired as at the first two corners.

2.8. *Rapid Expansion and Bulge.*—Up to the fourth corner the expansion ratio is 8·5 : 1, leaving only 1·4 per cent of the kinetic energy in the working-section to be recovered. However, it was felt that a larger contraction ratio was desirable to obtain low turbulence in the working-section, and to keep down the power losses in the smoothing screens. This was obtained by a means of a rapid expansion made effectively at constant pressure, thus maintaining a good velocity distribution[3]. The expansion is done through three stainless-steel wire-gauze screens (30 wires, of diameter 0·0095 in. per in.) at 3-ft spacing. The first of these screens is in one piece, the other two are of three strips brazed together.

The screens are square in shape with the corners outside the octagon of the tunnel section blanked off with fabric. They are fitted inside sealed boxes (Fig. 7) and are rigidly attached on two adjacent sides and spring-loaded on the other two sides. The slots in the tunnel walls through which the screens pass are shown in Fig. 8.

In the maximum section nine further screens (20 wires, of diameter 0·017 in. per in.) of phosphor bronze, manufactured in one piece, are fitted. These screens are removable, running on tracks at top and bottom. All the screens were in position throughout the work described in this report. As with the other screens they fit in sealed boxes and are spring-loaded on two sides. Fig. 9 shows the fixing and sealing at the side of the tunnel through which the screens are removed.

2·9. *Contraction Cone.*—Owing to changes in design made in the light of model tests after the main dimensions of the tunnel had been fixed, the contraction cone is shorter than is perhaps desirable. The middle part of the contraction is a frustrum of an octagonal pyramid with an angle of 100 deg between opposite walls. The initial and final parts were designed on the basis of model tests to give a monotonic pressure gradient along the walls. A change of section shape from a regular octagon to the irregular octagon of the working-section is made in the final part of the contraction.

2.10. *Speed Control.*—To avoid the time lags caused by the inertia of the fan and main motor, which occur in the normal type of speed control, a system operating independently of the fan has been installed. This consists of a duct by-passing the working-section, which takes up air just

downstream of the fan and discharges into the first diffuser (Fig. 10). The exit is provided with a flap operated through a worm and quadrant by an electric motor (Fig. 11). The motor can be controlled either by hand or from the automatic manometric balance. A sketch of the control circuit is given in Fig. 12.

The flap is mass-balanced, and is also balanced aerodynamically by a second flap attached to it, to opposite sides of which pressures from the by-pass duct and the tunnel are fed.

3. *Preliminary Flow Observations.*—Before any measurements were made in the tunnel an investigation of the flow was made by means of the observation of fine silk streamers. For the most part the flow was satisfactory and no signs of separation were found. The straighteners downstream of the fan were under-correcting the rotation imparted by the fan, to the extent of 20 or 30 deg near the walls at the downstream end of the second diffuser. This swirl affected the flow over the turning vanes at the third corner, causing a partial stall of the concave surface at the upper ends, and of the convex surface at the lower ends. Sheet-metal extension pieces fitted to the trailing edges of the straighteners eliminated the swirl and consequent stall.

Tufts attached to the trailing edges of the turning vanes showed that no alterations were required to the setting of the trailing-edge flaps, which were all set parallel to the tunnel centre-line.

No separation could be found in the rapid expansion but a region of flow reversal occurred on the concave walls at the start of the contraction when all nine damping screens were fitted. It was found later that this separation was absent when only two (the first and last) damping screens were fitted, but was present again when the last one was removed.

4. *Conditions in Working-Section.*—4.1. *Velocity Distribution.*—The distribution at three speeds is given in Fig. 13. Apart from the boundary layer on the tunnel walls the maximum variation in speed is $\pm\frac{1}{4}$ per cent. It was found that the setting of the speed control flap had no effect upon the distribution.

4.2. *Static-Pressure Gradient.*—The static-pressure gradient was measured by means of a tube 1 in. diameter and length 13 ft with pressure tappings at 1 ft spacing. The tube was suspended in the tunnel by a system of wires. The static pressure, expressed relative to the pressure measured at the hole-in-side nozzle in terms of $\frac{1}{2}\rho U_0^2$, where U_0 is the velocity at the centre of the working-section, is plotted in Fig. 14. The results for one speed only, 240 ft/sec are given. At other speeds the curves are similar. Some measurements were made with different settings of the speed control flap. The setting had no effect upon the static pressure.

There is a rapid decrease of static pressure along the initial stages of the working-section, attributed to the meaning out of the distribution in the final stages of the contraction cone, where there are high-speed regions on the fillets. A rough test using ' creeper ' static-pressure tubes on the fillets showed that the velocity there was about 5 per cent higher than at the centre.

As will be seen by comparing the curves for the observation room sealed and open, the magnitude of the flow into the tunnel through the vent holes at the end of the working-section has some effect upon the static-pressure gradient. At the time the measurements were made, the leaks from the tunnel circuit with the observation room open were considerably worse than the leaks into the ' sealed ' observation room.

The mean pressure gradient along the rear part of the working-section is $-0{\cdot}0025(\frac{1}{2}\rho U_0^2)$ per ft with the observation room open and $-0{\cdot}0020(\frac{1}{2}\rho U_0^2)$ per ft with the room sealed. Due to an error in the design calculations the expansion along the fillets is inadequate and should be about three times its present value. The following table gives the rate of expansion and pressure gradient in three other R.A.E. tunnels, and the rate of growth of the boundary-layer displacement-thickness, calculated from these figures.

TABLE 1

Tunnel	$\frac{\Delta A}{lx}$	$\frac{d}{dx}\left(\frac{p}{\frac{1}{2}\rho U_0^2}\right)$/ft	$\frac{d\delta^*}{dx}$	$R = \frac{U_0 x}{\nu}$
No. 1, $11\frac{1}{2} \times 8\frac{1}{2}$ ft	0·0018	0·0003	0·0015	2×10^7
No. 2, $11\frac{1}{2} \times 8\frac{1}{2}$ ft	0·0021	0·0004	0·0016	4×10^7
High Speed	0·0037	0·0017	0·0018	4×10^7
4×3 ft Observation Room Sealed ..	0·0006	—0·0020	0·0014	2×10^7

where ΔA area increase along working-section,
x length of working-section,
l perimeter of working-section,
p static pressure.

The mean value of 0·0016 for $d\delta^*/dx$ agrees fairly well with the latest information[4] on boundary-layer growth along a flat plate, which gives $d\delta^*/dx = 0{\cdot}002$ at 60 ft/sec.

4.3. *Steadiness of Flow.*—4.3.1. *Total head.*—In Fig. 15 the results of measurements, at two wind speeds, of the fluctuation of total head in the working-section and of fan speed are plotted. The total head was measured relative to atmosphere using a pitot-tube of 0·2 in. inside diameter, connected by about 6 ft of rubber tubing of the same bore to a Betz manometer. The method used to measure fan speed was that described in R. & M. 2424[1], consisting of a potentiometer across a high-tenstion battery balancing the mean output of the tachometer generator attached to the fan shaft, with the deviation measured on a millivoltmeter. The manometer and millivoltmeter were photographed at intervals of $2\frac{1}{2}$ sec over a period of 50 sec.

Table 2 gives values of standard deviation (the mean for both wind speeds) deduced from the results together with the values obtained for the R.A.E. No. 2, $11\frac{1}{2} \times 8\frac{1}{2}$ ft Tunnel in its final condition at 350 ft/sec (egg-box in second diffuser, honeycomb and three screens in the settling chamber).

TABLE 2

Tunnel	Total Head $\frac{\sqrt{(\Delta h)^2}}{h}$	Fan Speed $\frac{\sqrt{(\Delta \text{ r.p.m.})^2}}{(\text{r.p.m.})}$
4×3 ft	0·0006	0·00014
No. 2, $11\frac{1}{2} \times 8\frac{1}{2}$ ft	0·0014	0·00003

It is difficult to define a standard deviation for the fan speed because of the steady creep, which is probably genuine, not caused by drop in output of the high-tension battery, and must be attributed to temperature effects either on the power absorbed by the fan or on the motor itself. The deviation given above includes this creep. Even so the fluctuation in total head is greater than that appropriate to the fluctuation in fan speed and indicates that the resistance of the tunnel circuit varies with time. The total head fluctuations are less than half those of the No. 2 $11\frac{1}{2} \times 8\frac{1}{2}$ ft Tunnel.

4.3.2. *Direction.*—Some observations were made of the variation in pitch of the flow through the working-section using a light aluminium cone of $\frac{1}{2}$-in. side and included angle 60 deg, attached to fine silk streamer about 7 ft long. The results were inconclusive quantitatively, the streamer oscillating about $\pm 0{\cdot}1$ deg with the mean position steady.

5. *Velocity Distribution in Return Circuit.*—Vertical and horizontal traverses through the tunnel centre-line were made at each of six stations (Fig. 1) round the tunnel circuit with a more complete traverse ahead of the fan. The traverses were made with all the screens fitted, the by-pass flap closed and the temporary extension pieces fitted to the straightener vanes. The results are plotted in Fig. 16. The velocity is expressed in terms of the mean velocity for the station (U_{mean}) and the static pressure is given relative to the static pressure on the tunnel centre-line in terms of $\frac{1}{2}\rho(U_{\text{mean}})^2$.

Fig. 16a, giving the flow distribution at the end of the first diffuser, confirms the results of model tests[5], which showed that any tendency to flow separation would be avoided in a diffuser of 5 deg cone angle. The velocity profile shows a peak in the centre of about $1{\cdot}4U_{\text{mean}}$, which is of the same order as found in the model tests for a diffuser with uniform entry flow. (It is likely that the peak velocity is increased by the thickened boundary layer caused by the intake of low energy air at the vent holes compensating for that lost through leaks). However, the flow is symmetrical about the centre-line and shows no sign of instability. The drop in total head from the working-section to the centre portion of the traverse is $0{\cdot}3$ per cent of the dynamic head in the working-section.

The velocity contours of Fig. 16b show the flow approaching the fan. The distribution is nearly symmetrical about a horizontal centre-line but has an asymmetry about the vertical with the higher velocity on the inside of the circuit. This is probably the effect of the wake from the large fairing round the fan shaft bearing at the first corner. The individual wakes of the turning vanes are apparent.

In the second diffuser the flow is strongly influenced by the presence of the fan. Fig. 16c shows the distribution 4 ft behind the tail of the fan boss fairing. The effect of the boss is to reduce the velocity at the centre to half the mean velocity. The variation in static pressure across the tunnel indicates the presence of a rotation which was found to arise from swirl near the surface of the tail of the fan boss fairing.

The reduced velocity at the centre persists right round to the screens (Fig. 16g), but the static pressure is uniform by the end of the second diffuser (Fig. 16e). The static pressure downstream of the fourth corner is higher in the centre than near the walls by some 20 per cent of the local dynamic head. This can be attributed to the speeding up of the flow on the walls approaching the rapid expansion and means that the distribution of total head is not as good as might be expected from the velocity distribution.

When the temporary flaps on the straighteners were replaced by more permanent fittings the swirl in the second diffuser was modified. The seven temporary flaps probably deflected differently under load, and the effect of the more rigid fittings is an over-correction of the fan rotation. This amounts to about 10 deg on the walls at the end of the second diffuser. The resulting flow is more uniform as shown in Fig. 17.

The asymmetry at the end of the second diffuser can be reduced slightly by differential adjustment of the flaps on the turning vanes at the second corner. The effect is, however, largely masked by the swirl and it was decided to leave the flaps at their original setting.

6. *Velocity and Total-Head Distributions in Bulge.*—6.1. *Method of Measurement.*—The measurements required an instrument which would record wind speeds down to 5 ft/sec and which would be insensitive to yaw. A Sperry double-venturi, when fitted with a central pitot-tube, satisfied these requirements. This instrument has been described fully elsewhere[6] but for the sake of completeness a sketch is given in Fig. 18 and Figs. 19 and 20 show the results of a calibration in the R.A.E. Seaplane Tank together with points obtained in the tunnel using a vane anemometer. The pressures were read on a tilting Chattock Manometer.

The venturi was mounted across a diagonal of each tunnel section on two taut wires passing through tubes attached to it. It was traversed across the tunnel by a cord which was marked at appropriate intervals and led to a pulley outside the tunnel. The sections at which traverses were made are shown in Fig. 21. The lines mark the plane of the exit of the venturi since the pressure registered by the static ring will be controlled mainly by the pressure at the exit.

The tunnel was run throughout at a speed of 240 ft/sec in the working-section.

6.2. *Results and Discussion.*—6.2.1. *Velocity distribution.*—The velocity distribution at each station is given in Fig. 22 the velocity being referred to that at the centre (U_c). The venturi readings have been corrected for estimated yaw by the curve of Fig. 19.

The velocity distribution improves through the screens in the expansion and downstream of the third screen is constant to within about $\pm$ 3 per cent. Throughout the expansion the velocity is higher in the upper half of the diagonal which is also the outside of the tunnel circuit. This agrees with the measurements before the expansion (Fig. 16g) which show higher velocity at the top and outside of the section.

The velocity profile deteriorates through the smoothing screens and downstream of all the screens (Fig. 22d) has a peak in the centre of the order of 10 to 15 per cent above the mean. This is produced by the curvature imposed on the streamlines by the walls of the contraction. There is a curious peak in velocity near the wall at one side. A traverse made at right-angles showed something similar but not quite so marked. This peak is associated in some way with the separation occurring in the contraction but the complete mechanism of the flow is not fully understood. To try to improve the flow, fillets were fitted on two adjacent sides of the contraction increasing the radius of curvature from 4·3 to 7 ft. These fillets reduced the extent of the flow reversal but did not cure it completely.

6.2.2. *Total head.*—The total head, referred to that at the centre, across the various sections is plotted in Fig. 23 in terms of $\frac{1}{2}\rho U_M^2$, where U_M is the mean velocity at the section calculated from the velocity in the working-section.

Through the expansion there is a progressive rise in total head near the walls relative to that at the centre. This can be explained as the combined effect of the resistance of the gauzes and the curvature of the streamlines. For example, the streamlines through the nine smoothing screens are concave towards the centre-line, leading to an increased static pressure near the walls and a reduction of velocity there. Consequently the pressure drop through the screens is less near the walls than at the centre. The total head downstream of the screens is therefore high near the walls, although due to the static-pressure gradient across the section the velocity is low near the walls.

The resistance coefficients calculated from the measurements are 2·5 for the expansion screens and 3·6 for the smoothing screens. These values are obtained as the difference of two large quantities so that their agreement with the general data[7] can be considered satisfactory.

6.2.3. *Comparison with model tests.*—The expansion and contraction cone were designed on the basis of the results of a series of tests on models of about $\frac{1}{13}$th scale. The results of the first tests have been reported by Squire and Hogg[3]. In order to facilitate the measurements, the model tests were made at higher wind speeds than in the full-scale tunnel. This led to lower values for the pressure-drop coefficient of the gauzes at the higher Reynolds number and the velocity distributions obtained full scale are somewhat better than in the models. Since the geometry of model and full scale is the same, the pressure gradients are similar.

One major difference between model and full scale is the existence of the return flow in the contraction cone which was not found on the model. A plausible explanation is that at the low full-scale wind speed the flow through the gauzes becomes laminar leading to a laminar separation in the adverse pressure gradient at the start of the contraction, whereas the boundary layer may have been turbulent on the model.

The differing boundary layer conditions might also explain the dependence of the separation upon the number of damping screens, mentioned in section 3.

7. *Tunnel Power Factor.*—The tunnel power factor is defined as

$$\text{Input power to fan} / \tfrac{1}{2}\rho A_0 U_0^3$$

where A_0 area of working-section,

U_0 wind speed in working-section,

ρ air density in working-section.

The results of measurements are plotted in Figs. 24 and 25. The power input to the fan was determined from the power supplied to the fan motor which was assumed to be 90 per cent efficient. The apparent large scale effect in Fig. 24 is thus probably not entirely genuine, some of the effect will be due to changes in the efficiency of the motor.

The difference between the values of the power factor for the observation room sealed and open is caused by the large leaks in the tunnel with the working-section at atmospheric pressure. It has been found almost impossible to seal the tunnel circuit, particularly round the removable screens, and it has been decided that the normal operation of the tunnel shall be at a reduced pressure in the working-section, with the observation room sealed and the return circuit vented to atmosphere. At the time of the power-factor measurements the leak area into the observation room deduced from pressure measurement was 0·4 sq ft.

The following table gives an analysis of the losses round the tunnel circuit deduced from the results of traverses which were made with the observation room open.

TABLE 3

Analysis of losses with observation room open

Measured power factor at 250 ft/sec = 0·32.

Section	Power-factor contribution
Contraction cone, working-section and first diffuser (including leak losses)	0·159
First and second corners	0·040
Second diffuser	0·009
Third and fourth corners	0·004
Screens	0·064
Fan (assumed 90 per cent efficient)	0·031
Unaccounted for	0·01
Total power factor	0·32

The main feature of this table is the large contribution of the working-section and first diffuser. This contribution includes the effect of the low energy air flowing into the vent holes at the end of the working-section, to compensate for the leak losses in the return circuit, which produces a thick boundary layer along the first diffuser. It is interesting to compare the measured power factor with what might be estimated in the design stage of a tunnel. The comparison is made in the following table using the power factor for the sealed observation room for which the leak loss is not so large. The assumptions made for each section of the tunnel are given, the general assumption of uniform flow across any section of the tunnel being made throughout.

TABLE 4

Estimation of loss with observation room sealed

Measured power factor at 280 ft/sec = 0·27.

Section	Assumptions		Power-factor contribution
Contraction cone and working-section	Flat plate turbulent $C_f = 0{\cdot}0026$		
	Contraction cone equivalent to 20 per cent of working-section	0·041	0·104
First diffuser	Loss coefficient 0·075	0·063	
First and second corners	Loss coefficient 0·08 per corner + skin friction loss on walls	0·02	0·030
Second diffuser ..	Loss coefficient 0·075		0·011
Third and fourth corners	As first and second corners		0·003
Screens	Estimated from Ref. 6		0·065
Fan	Efficiency = 90 per cent...		0·024
Unaccounted for ..			0·03
	Total power factor		0·27

Considering the assumption made of uniform flow across any section and the absence of any allowance for leaks the discrepancy of 0·03 is small. The conclusion is that the ordinary rough estimate of power factor is satisfactory if an allowance of 10 per cent is made to cover leaks etc.

The main difference between Tables 3 and 4 is in the loss along the working-section and first diffuser which is accounted for by the leaks. Other differences are due principally to the effect of non-uniformity of the flow.

8. *General Discussion.*—The deductions gained from experience with the 4 × 3-ft Tunnel which can be applied to the design of other (subsonic) tunnels are considered in turn beginning with the simpler ones.

8.1. *Diffuser Cone Angle.*—The final velocity distribution ahead of the first screen (Fig. 17b) could hardly be better. This is partly due to the use of a smaller diffuser angle than is usual, but is partly fortuitous in that the wake of the fan boss fairing has finally disappeared at this station. It seems that the diffuser cone angle (5 deg) used is a suitable value to eliminate any tendency to asymmetry in velocity distribution, but an artificially introduced asymmetry (section 5) will not normally be smoothed out.

8.2. *Corner Design.*—The use of cascades with a gap /chord ratio of $\frac{1}{4}$ is satisfactory in eliminating non-uniformity in the outflow. At the same time the pressure drop is not appreciably increased. It is recommended that cascades of this type should be used in future. No provision for adjustable trailing edges is necessary.

It has been found[8] that, at the first corner, thin plate vanes of the same dimensions are satisfactory and have a lower pressure drop.

8.3. *Pre-rotation Vanes and Straighteners.*—The experience acquired suggests that adjustable flaps on the trailing edges of the straighteners would be useful. In view of the uncertain radial velocity distribution in the stream it is considered that there is nothing to be gained by departing from the normal practice of using untwisted straighteners designed to remove only the mean swirl.

8.4. *Area Ratio at the First Bend.*—The ratio of the area of the cross-section at the first bend to the area of the working-section is an important feature. Its value should be chosen to ensure that the losses at the first two corners are a sufficiently small proportion of the total power losses in the tunnel. In most cases there is little justification for reducing the bend losses below say 10 per cent of the total power losses but they should be less than 20 per cent of the total. The value chosen represents a compromise between capital cost and running costs.

For the 4 × 3-ft Tunnel the choice of an area ratio of $2\frac{1}{2}$ at the first bend gives a loss at the first two corners of about 15 per cent of the total power loss. There would be little justification in using an area ratio greater than 3 unless the tunnel power factor were well under 0·2.

8.5. *Bulge and Contraction Cone.*—The operation of the bulge can be considered satisfactory. In fact it seems likely that screens of smaller resistance could be used without any deterioration in flow. The total-head variation across the maximum section is probably not of practical importance in this case with the large contraction ratio of the wind tunnel.

The contraction cone with monotonic increase in velocity along its walls to the value in the working-section is an ideal which cannot be fully attained in practice. In the present design there is some rise in pressure in the initial part of the contraction which leads to a boundary-layer separation. The initial stages of the contraction cone should be more gradual to obviate this. There are also regions of high velocity on the fillets just ahead of the working-section which do not produce any marked ill effects.

8.6. *Speed Control.*—The by-pass method of control fitted to the 4 × 3-ft Tunnel is satisfactory aerodynamically, and improvements to the electrical gear are being made to eliminate the defects which have been encountered.

Acknowledgment is due to E. G. Barnes, R. C. W. Eyre, D. A. Treadgold and P. E. Watts for assistance in the investigation.

REFERENCES

No.	*Author*	*Title, etc.*
1.	D. C. MacPhail, J. G. Ross and E. C. Brown	The No. 2, $11\frac{1}{2} \times 8\frac{1}{2}$ ft Wind Tunnel. R. & M. 2424. August, 1945.
2.	—	Design of Proposed 4 × 3-ft Wind Tunnel. R.A.E. Tech. Note Aero. 1362. A.R.C. Report 7323. January, 1944.
3.	H. B. Squire and H. Hogg ..	Diffuser Resistance Combinations in Relation to Wind-Tunnel Design. R.A.E. Report Aero. 1933. A.R.C. Report 7628. April, 1944.
4.	W. Tillmann	Investigations of some Particularities of Turbulent Boundary Layers on Plates. Reports & Translations 45. A.R.C. Report 9732. March, 1946.
5.	K. G. Winter	Tests of a Partial Model of the Proposed R.A.E. 4-ft × 3-ft Wind Tunnel. R.A.E. Tech. Note Aero. 1406. A.R.C. Report 7619. March, 1944.
6.	P. Brotherhood	An Investigation in Flight of the Induced Velocity Distributoin under a Helicopter Rotor when Hovering. R. & M. 2521. June, 1947.
7.	L. F. G. Simmons and C. F. Cowdrey	Measurements of the Aerodynamic Forces Acting on Porous Sheets. A.R.C. Report 8920. August, 1945.
8.	K. G. Winter	Comparative Tests of Thick and Thin Turning Vanes in the 4 × 3-ft Wind Tunnel. R. & M. 2589. August, 1947.

APPENDIX I

Automatic Speed Control

1. *Introductory.*—1.1. *Necessity for Control.*—It is necessary to have some form of speed control in a wind tunnel to correct for :—

(a) Variations in the power supply to the fan motor.

(b) Temperature effects on the tunnel and on the motor.

(c) Variations of the tunnel power factor caused by the change of the drag of models with incidence.

1.2. *Requirements of a Control.*—The three following requirements are suggested for a satisfactory control :—

(a) The range of operation to be sufficient to correct the normal speed deviations likely to be encountered.

(b) The rate of operation to be sufficiently rapid to avoid long delays in waiting for deviations to be rectified.

(c) There must be no ' hunting '.

1.3. *Type of Control.*—The possible means of controlling a tunnel fall into three main groups.

(a) The normal method of variation of the power supply to the fan motor.

(b) Artificial variation of the tunnel power factor.

(c) Variation of the flow through the working-section by altering the flow through an auxiliary duct by-passing the working-section.

The last type (c) has the advantage over (a) and (b) that, with suitable design of the by-pass duct, the fan operates under conditions which are sensibly independent of the flow through the by-pass duct, and hence the time lags, caused by the inertia of the motor and fan, and by the electrical inertia of the motor windings, are eliminated. The experimental control for the 4 × 3-ft Tunnel was, therefore, chosen to be of the last type. It is described in section 2.10.

2. *Operation of* 4 × 3-*ft Control.*—Figs. 20 and 21 show the speed range covered by the movement of the speed-control flap, and the speed deviations corresponding to the various signal lights operated by the manometric balance (Fig. 12). These results show that the signal lights and the flap range are well balanced and that the controllable speed range is adequate.

The requirements (b) and (c) of section 1.2 are interdependent since too rapid adjustment of the speed will lead to hunting. With the present installation, for which the rate of movement of the flap is independent of the speed deviation, hunting depends upon the following factors :—

(a) Rate of movement of flap.

(b) Magnitude of the ' dead-space '. The ' dead-space ' is the speed range over which no control is exercised by the manometric balance, and is indicated by two white signal lights (Fig. 21). The range corresponds to $\pm$ 0·03 per cent variation in speed, which is about one-quarter of the range usually used in tunnels at the R.A.E.

In addition, hunting depends upon the time lags caused by :—

(i) The manometric balance.

(ii) Acceleration and retardation of flap motor.

(iii) Inertia of the tunnel air.

Of these factors the one immediately controllable is (a), and attention has so far been confined to the variation of this. The rate of movement of the flap can be adjusted by the series resistance R in Fig. 12, and with suitable values of R, a control which is just satisfactory can be obtained, as demonstrated in Fig. 22.

The curves of Fig. 22 were obtained by adjusting the fan speed until the wind speed deviated by about 1 per cent from that set on the manometric balance, and recording the time for each change of the lights. The size of the peaks showing deviations is thus arbitrary. The difference between the upper and lower pairs of curves shows the effect of increasing R.

Difficulty was experienced, however, in that the speed-control flap was aerodynamically over-balanced, and the flap motor insufficiently geared down. Consequently at high tunnel speeds the control became asymmetrical in operation. Fig. 11 shows the alterations made to the flap, which reduced the over-balance by some 40 per cent.

Two further modifications have been made to the installation :—

(1) The reduction gear from the motor to the flap has been increased by 4 : 1.

(2) A variable shunt-resistance has been inserted across the motor armature. This enables the ultimate speed of the motor to be varied with little effect upon the starting torque and acceleration.

No records of the behaviour of the control under these conditions have been taken but general observation indicates that there is an appreciable improvement.

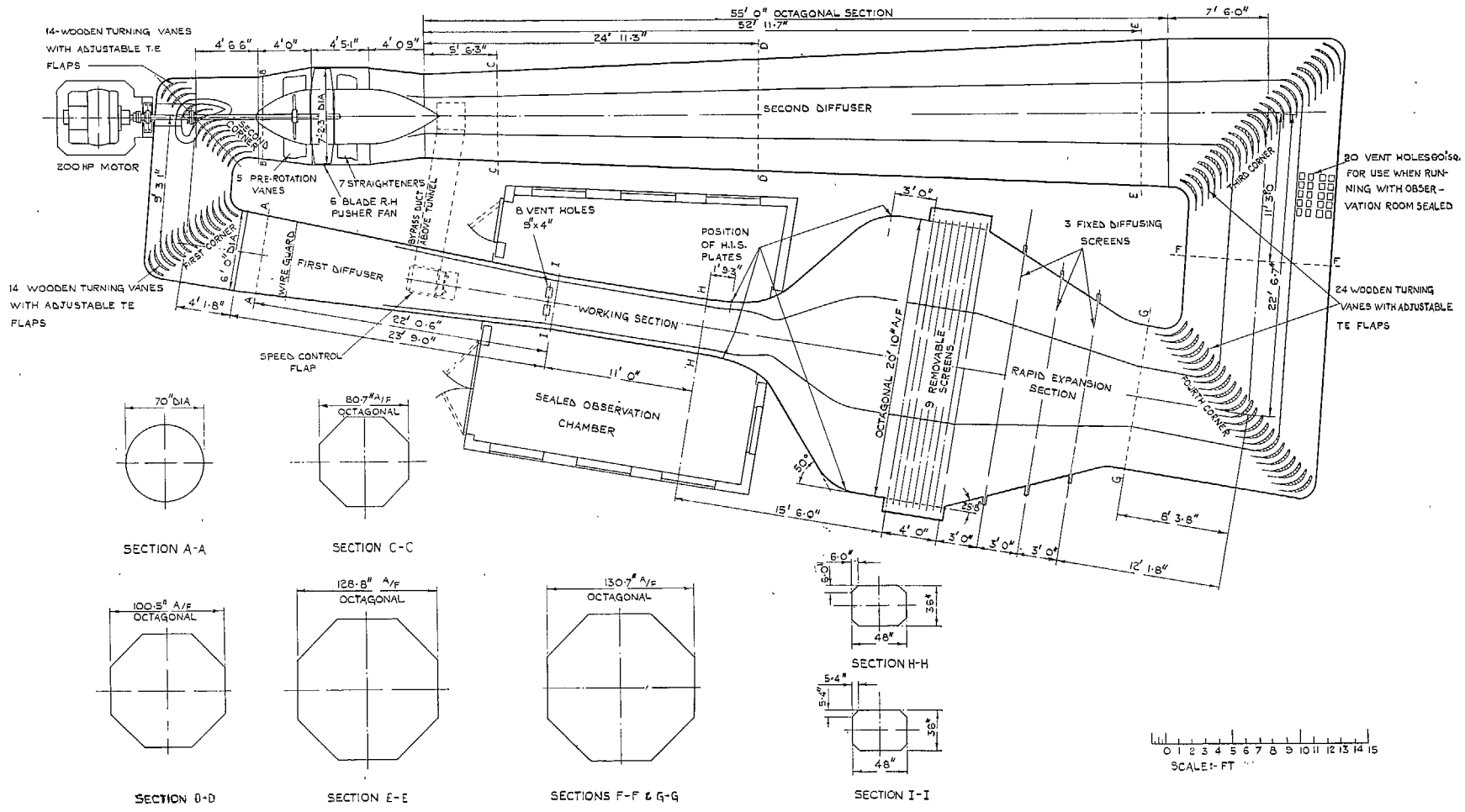

FIG. 1. 4 × 3-ft wind tunnel, R.A.E. Sectional plan on tunnel centre-line.

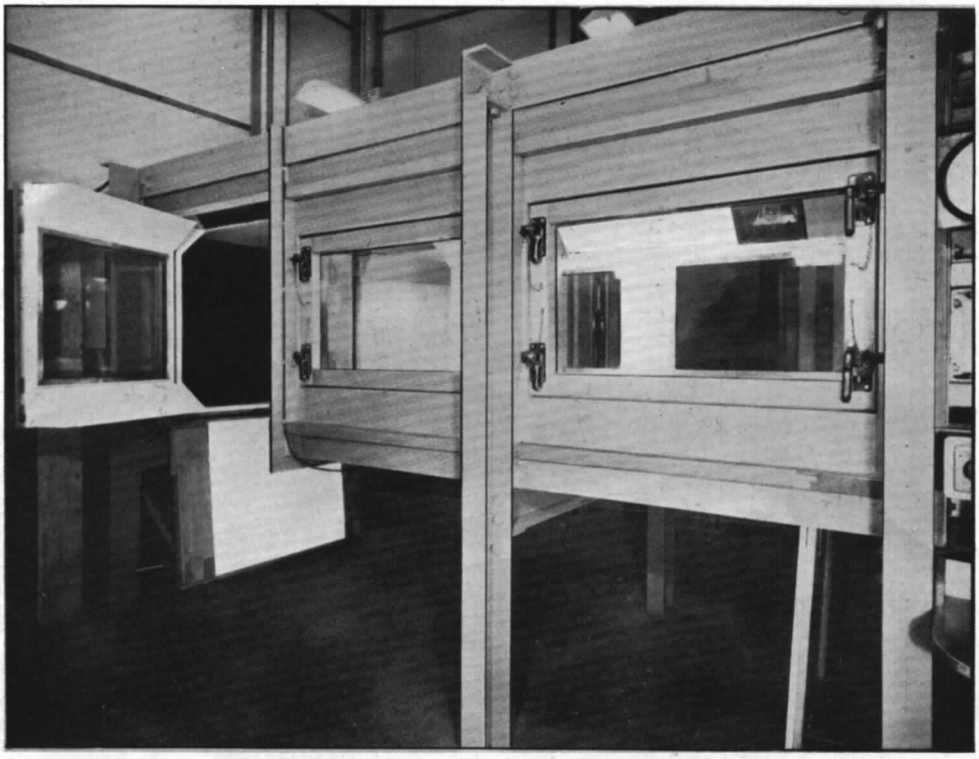

FIG. 2. Working-section showing access doors

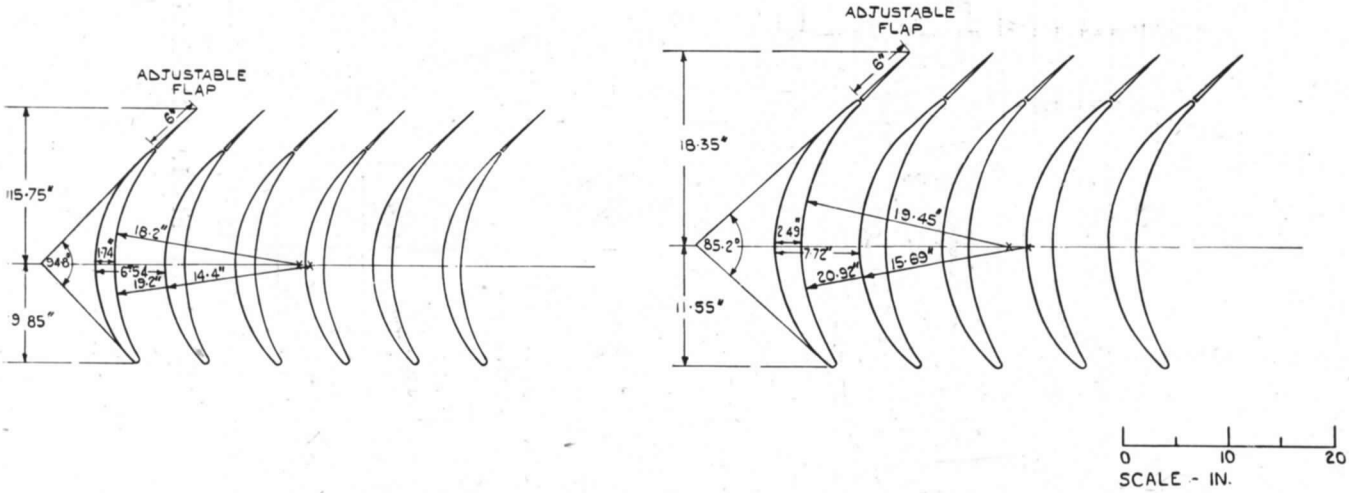

First and second corner: 14 turning vanes.

Third and fourth corner: 24 turning vanes.

FIG. 3.

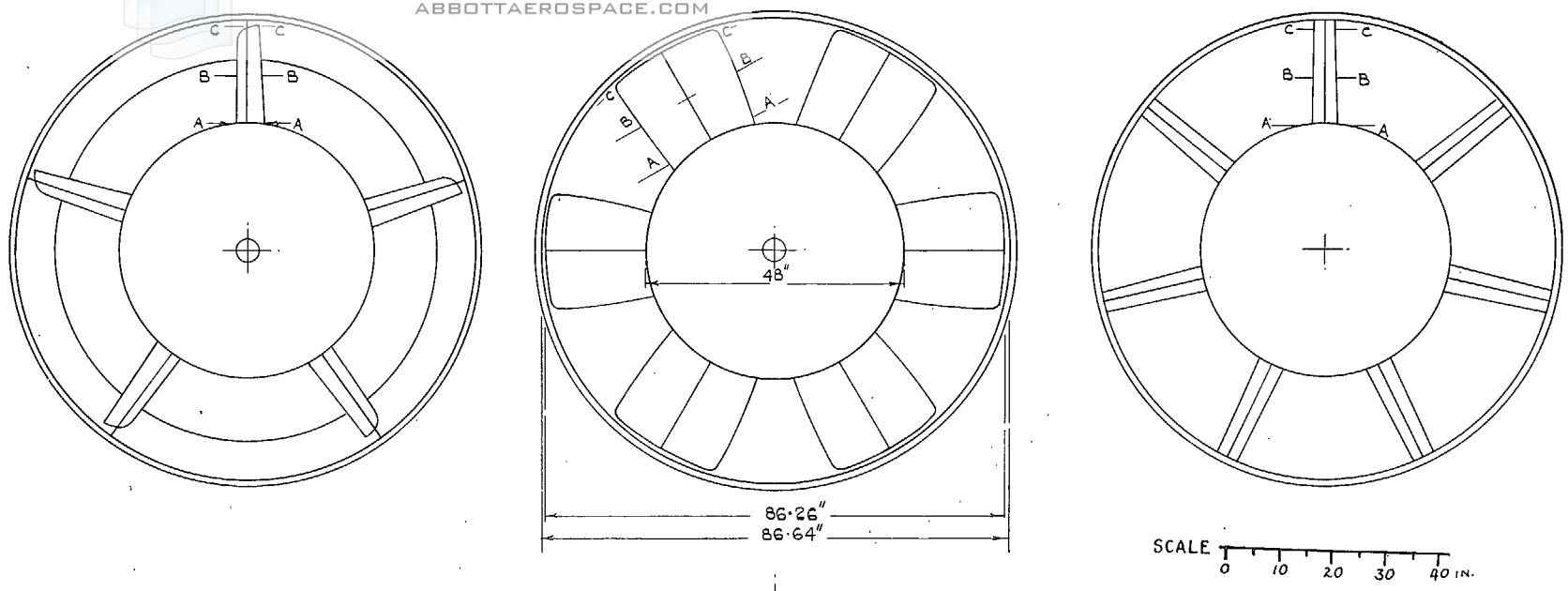

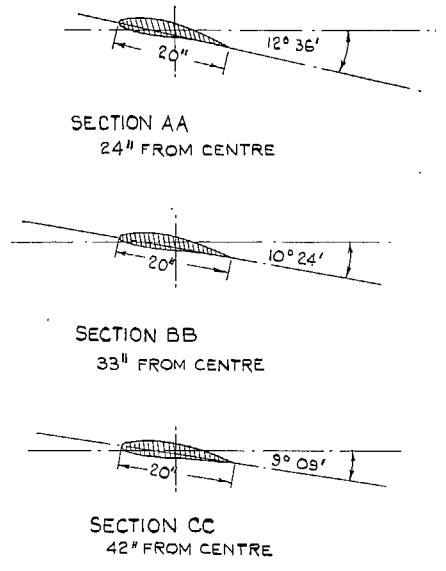

Pre-rotation vanes.

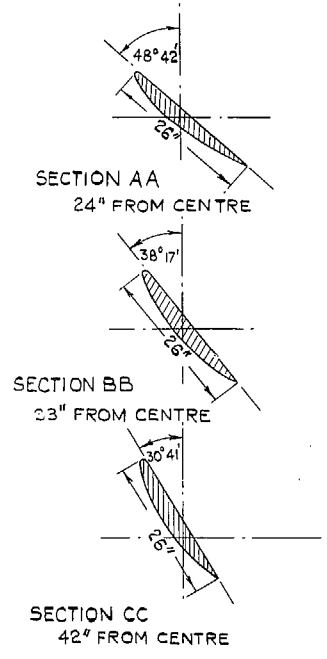

Fan.

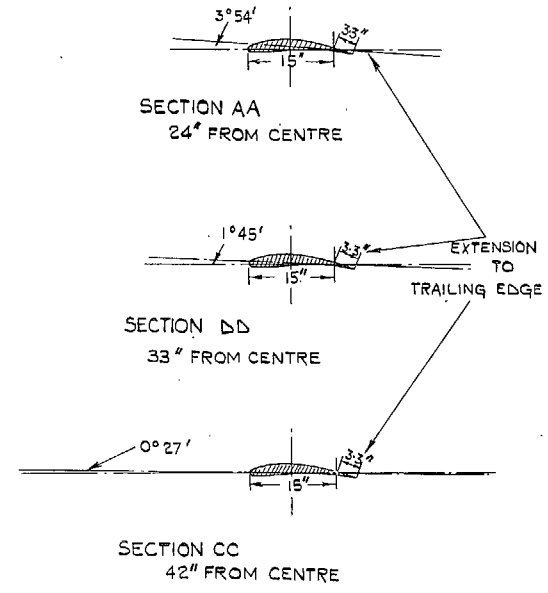

Straightener vanes.

FIG. 4. Fan installation.

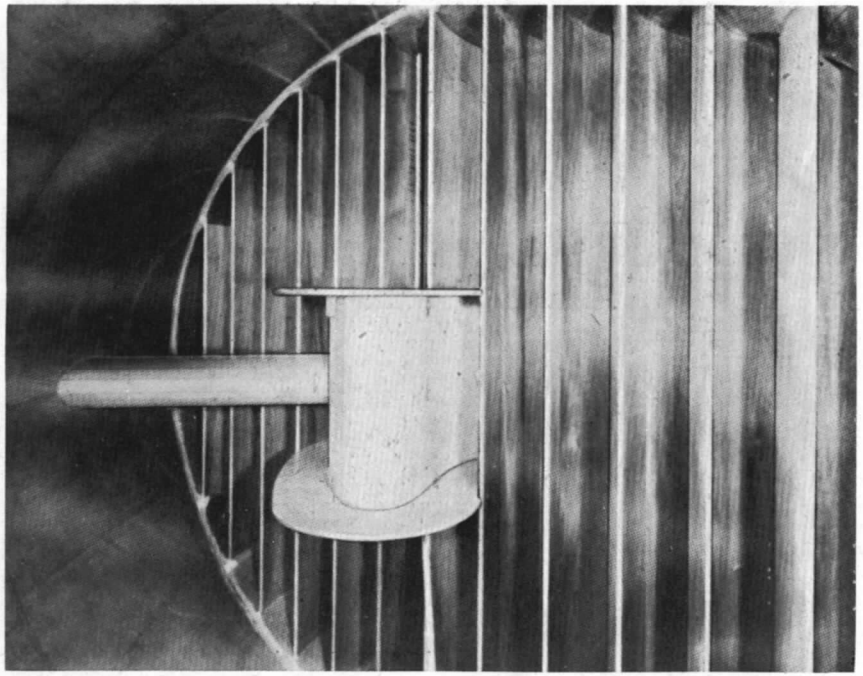

FIG. 5. Fairings over fan shaft and bearing at second corner.

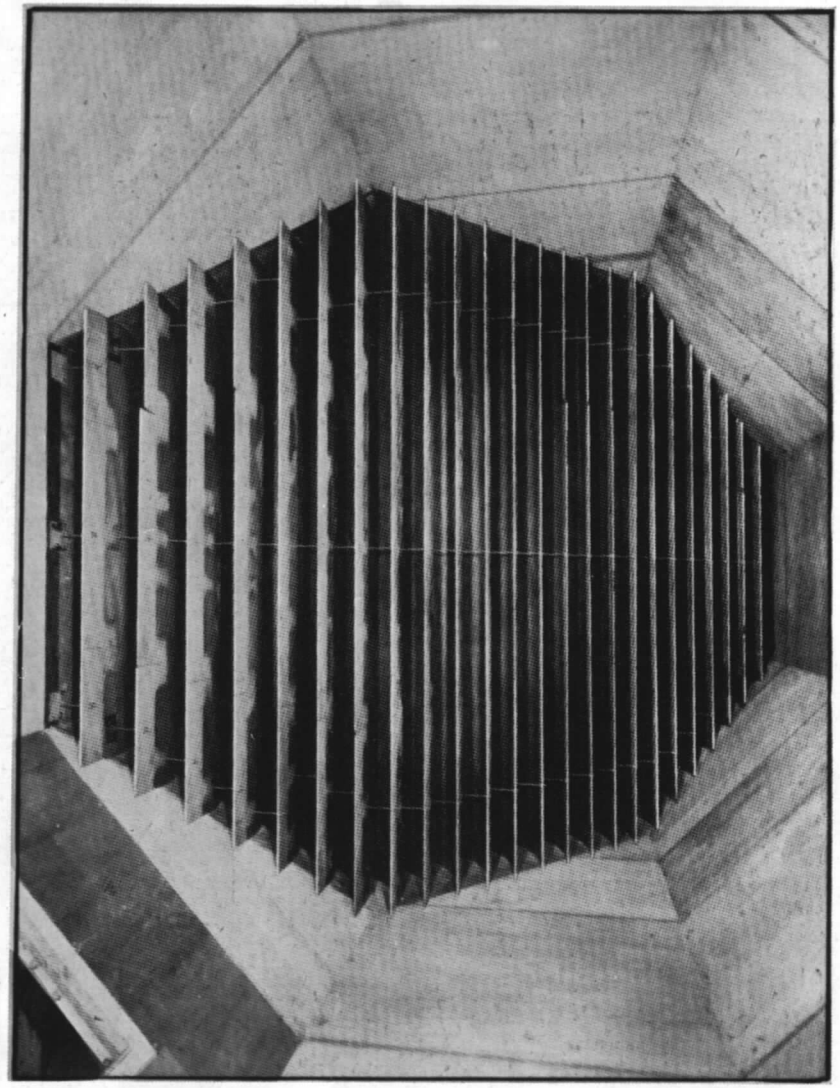

FIG. 6. Turning vanes at third corner showing adjustable flaps.

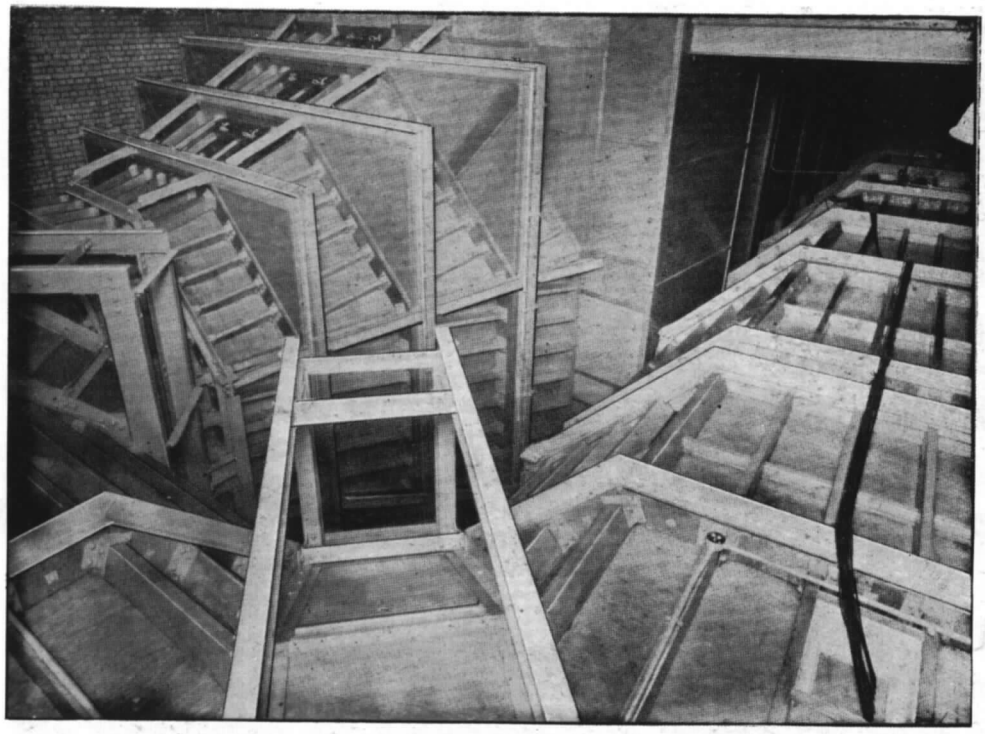

FIG. 7. External view of rapid expansion showing sealing boxes for screens.

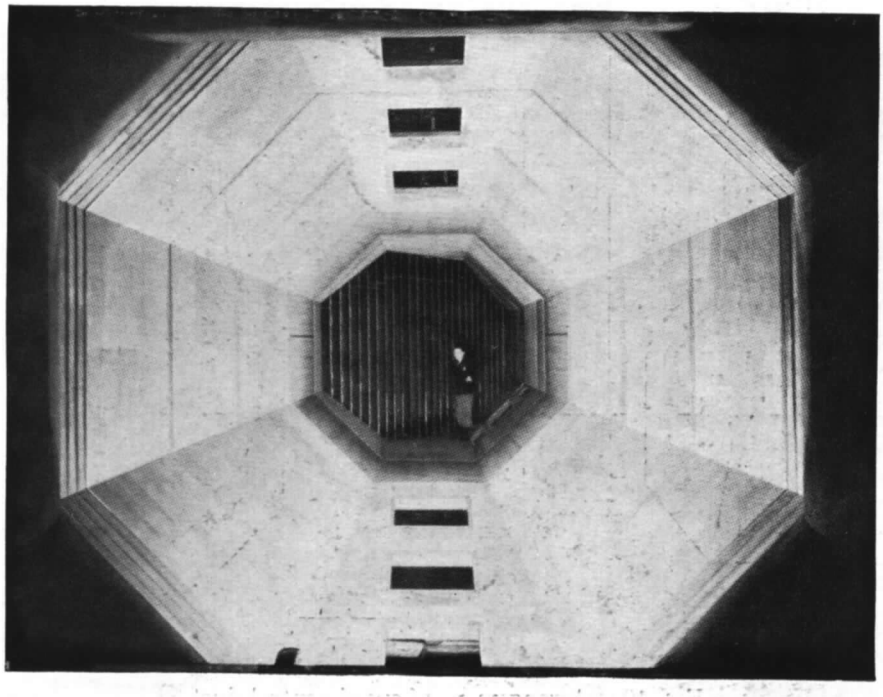

FIG. 8. View upstream from working-section showing slots for screens.

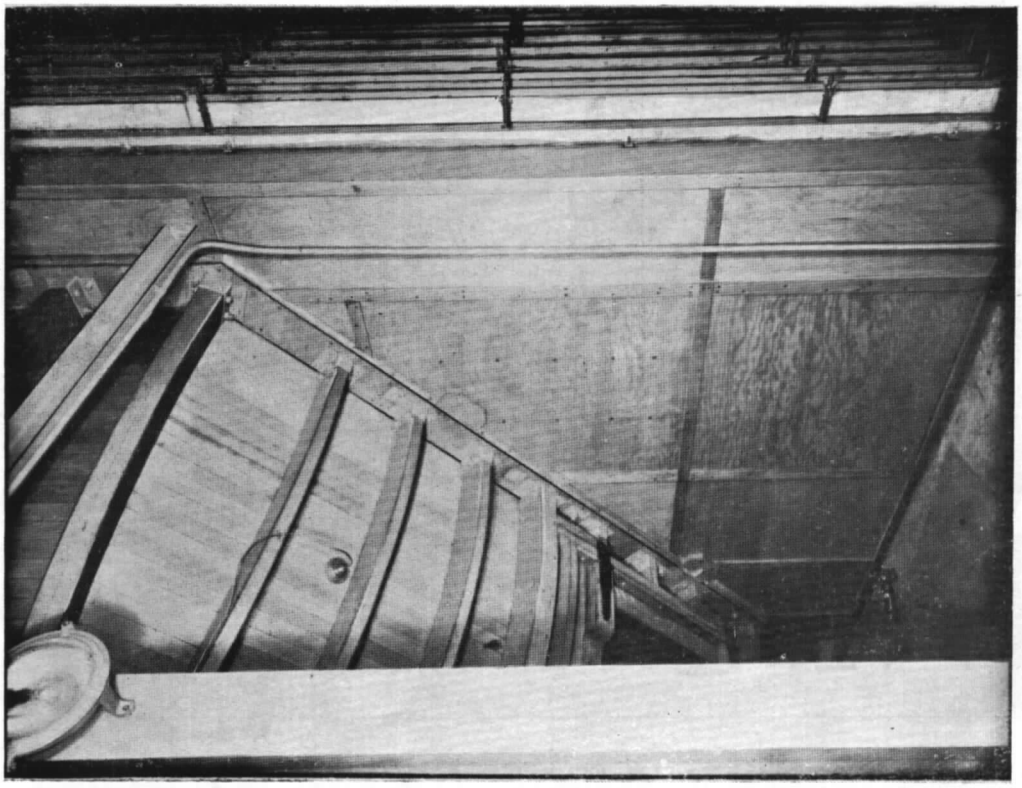

FIG. 9. Fixings for removable screens.

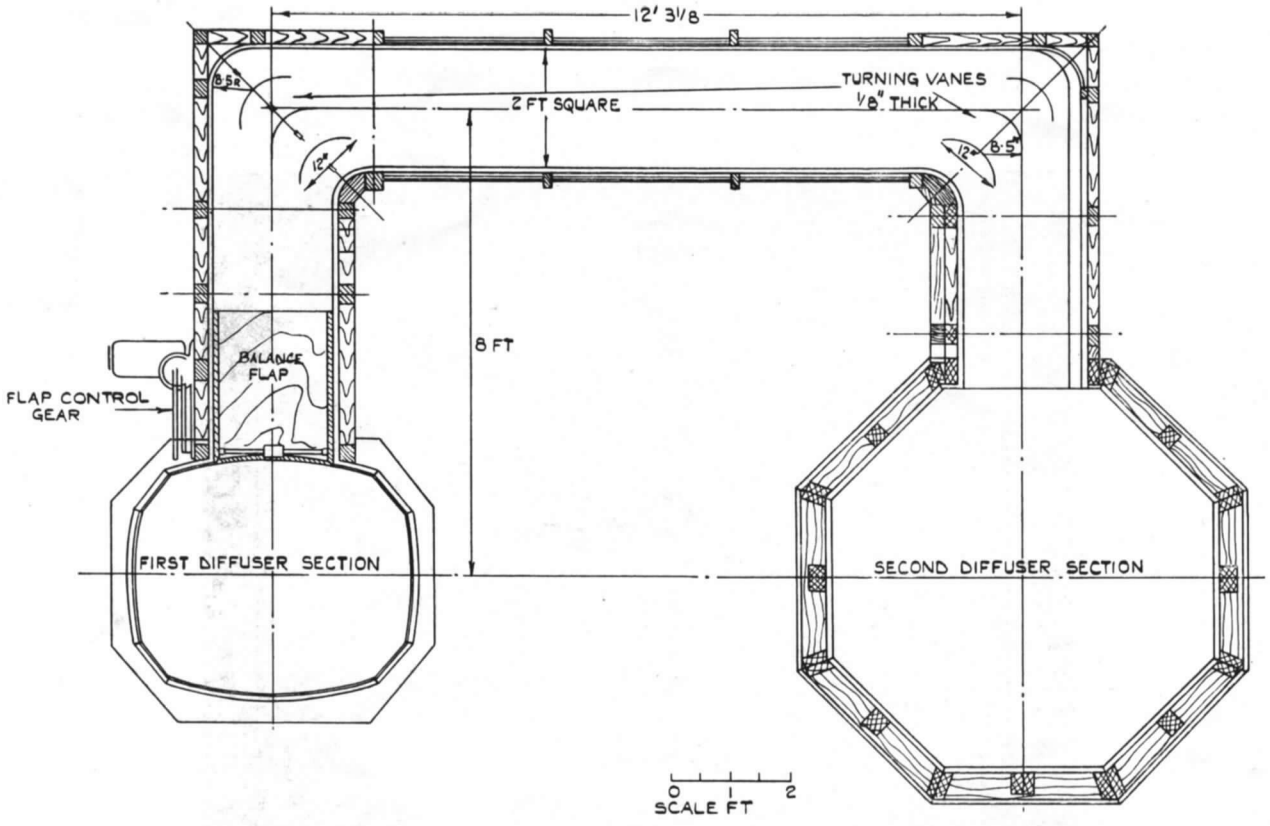

FIG. 10. Arrangement of speed-control duct.

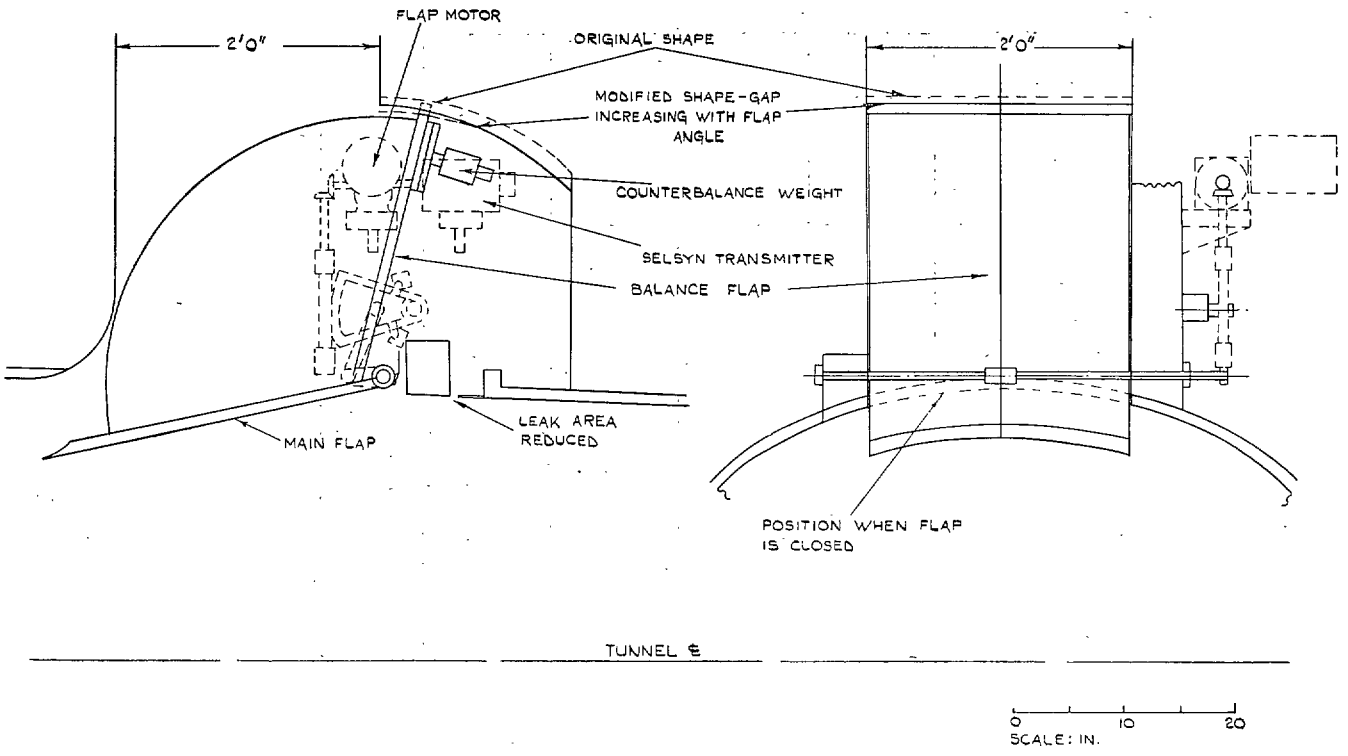

FIG. 11. Arrangement of speed-control flap.

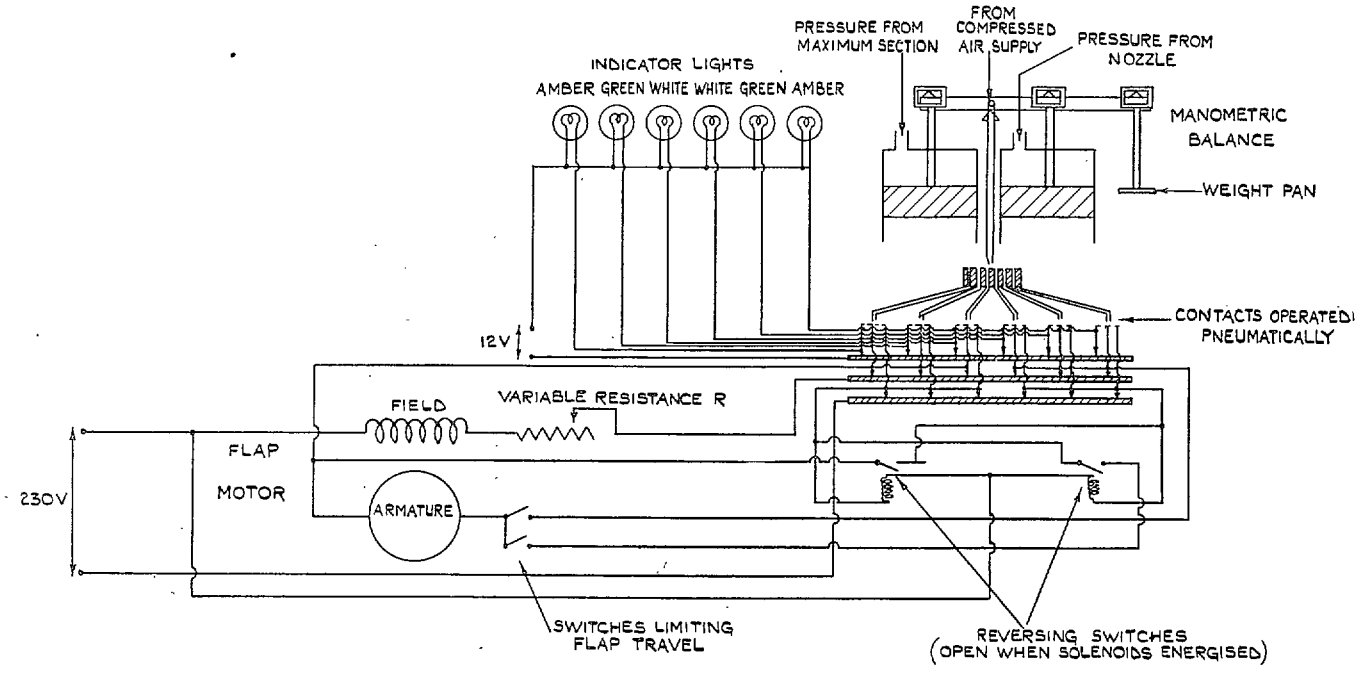

FIG. 12. Automatic speed-control system.

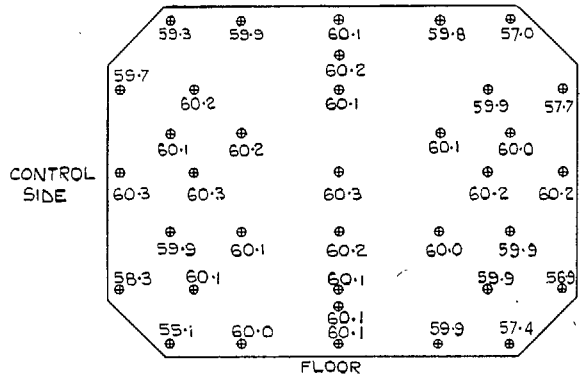

FIG. 13. Velocity distribution in working-section.

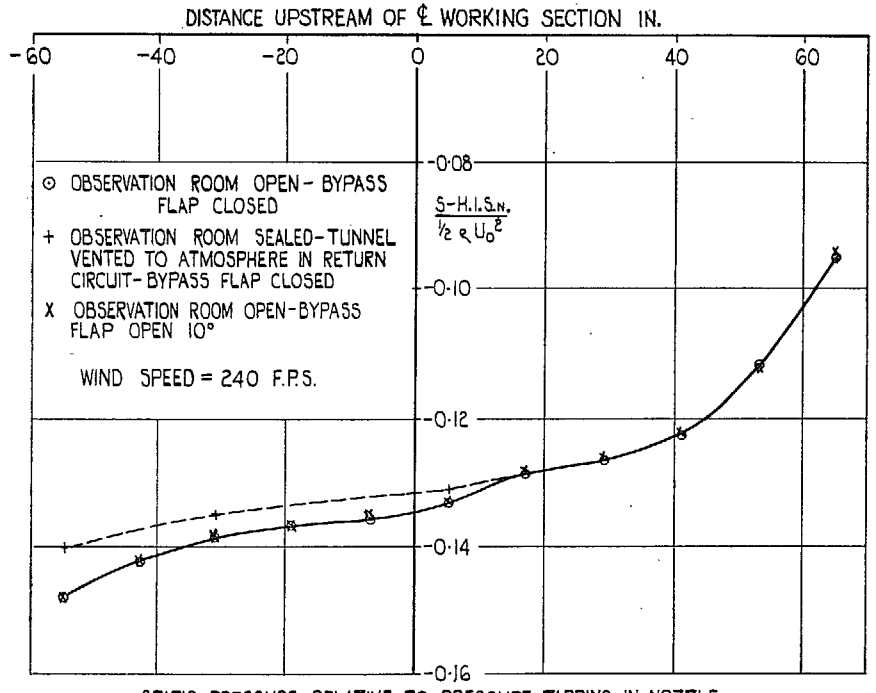

FIG. 14. Static-pressure gradient along working-section.

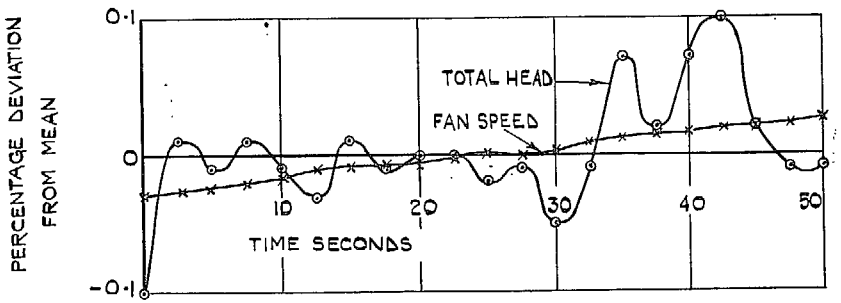

FAN SPEED ≑ 400 R.P.M. WIND SPEED ≑ 175 F.P.S.

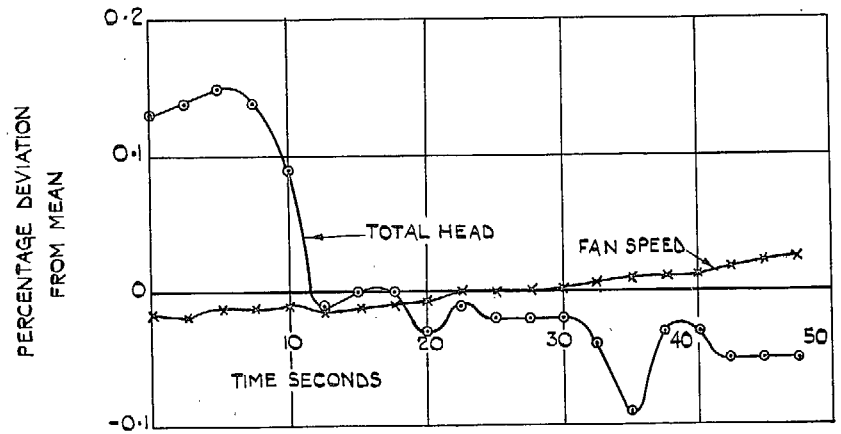

FAN SPEED ≑ 565 R.P.M. WIND SPEED ≑ 240 F.P.S.

FIG. 15. Fluctuations of total head in working-section and of fan speed.

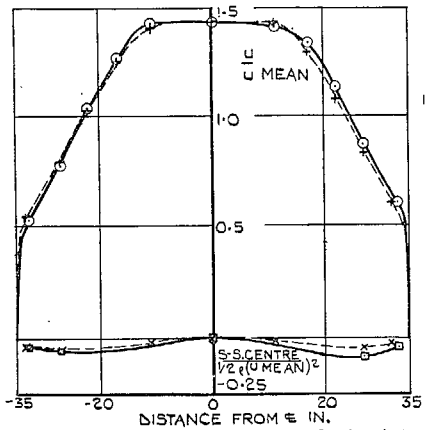

FIG. 16(a)

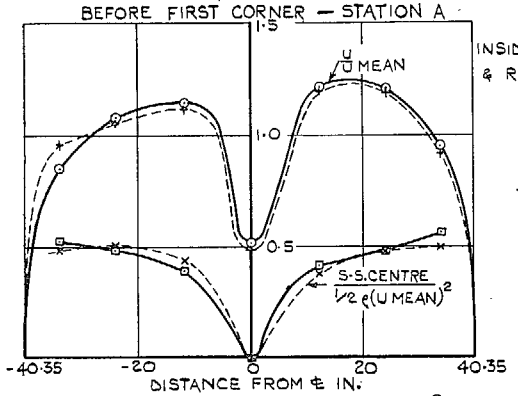

FIG. 16(c)

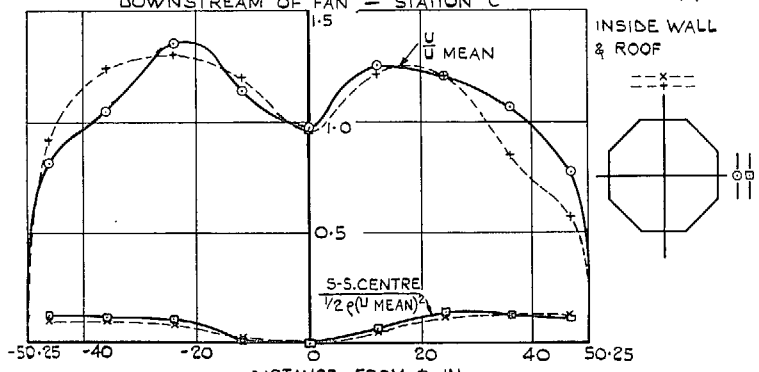

FIG. 16(d)

FIG. 16a, c, and d. Flow in return circuit.
(Temporary extensions fitted to fan straightener vanes. All screens fitted. By-pass flap closed. $U_0 = 250$ ft/sec).

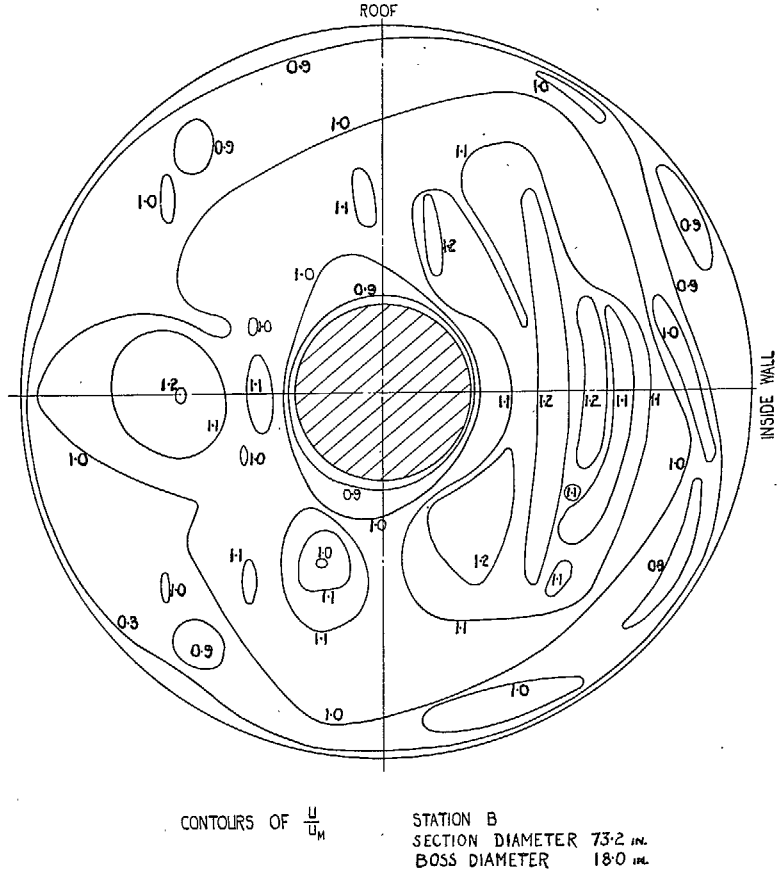

FIG. 16b. Velocity distribution approaching fan.

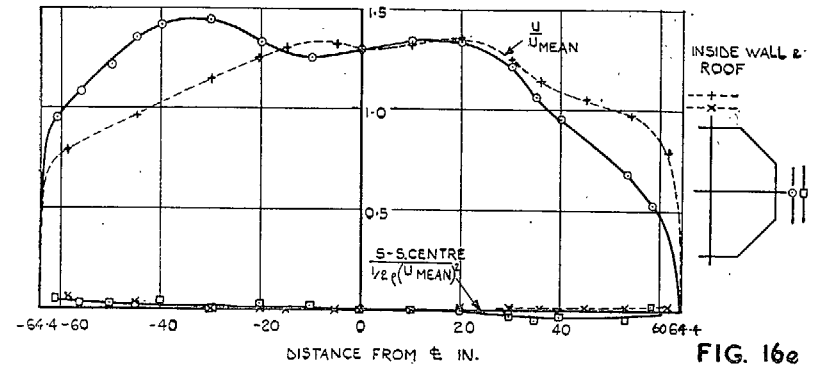

FIG. 16e

UPSTREAM OF THIRD CORNER – STATION E

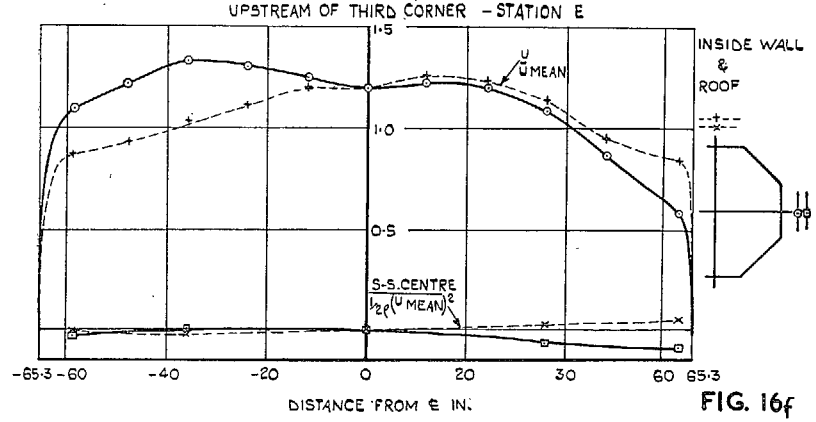

FIG. 16f

BETWEEN THIRD & FOURTH CORNER – STATION F

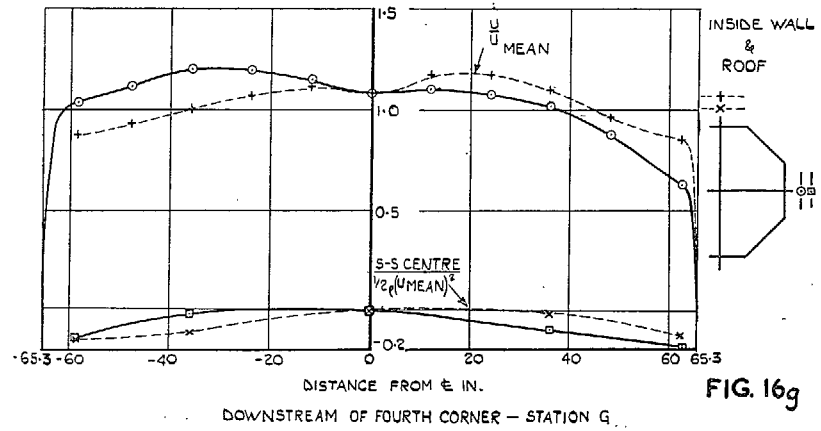

FIG. 16g

DOWNSTREAM OF FOURTH CORNER – STATION G

FIG. 16e, f, and g. Flow in return circuit.
(Temporary extensions fitted to fan straightener vanes. All screens fitted. By-pass flap closed. $U_0 = 250$ ft/sec).

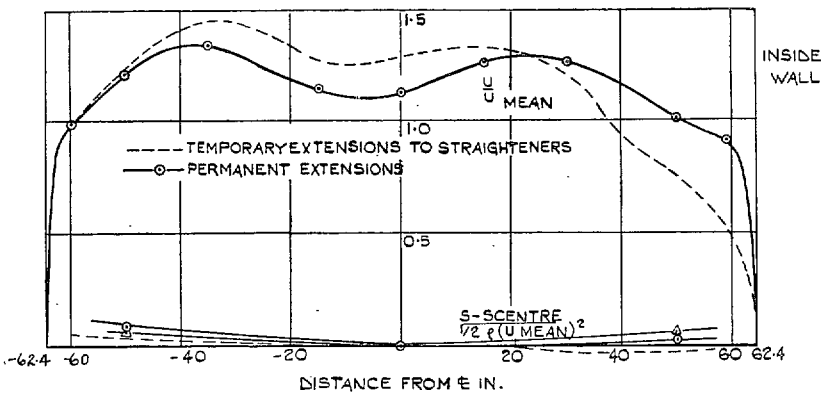

FIG. 17a. Horizontal traverse upstream of third corner : Station E.

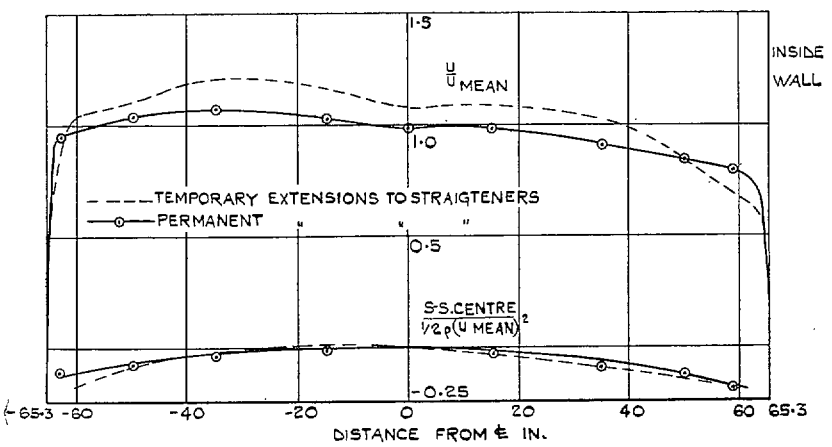

FIG. 17b. Horizontal traverse downstream of fourth corner : Station G.

FIG. 17. Effect of straightener vanes. Flow in return circuit.
(All screens fitted. By-pass flap closed. $U_0 = 250$ ft/sec).

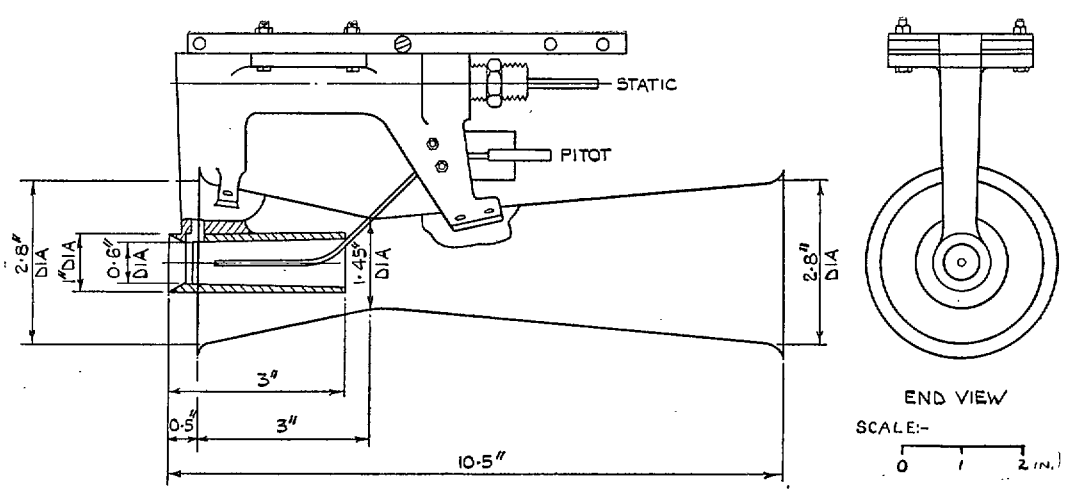

FIG. 18. Cross-section of modified double-venturi pitot-static tube.

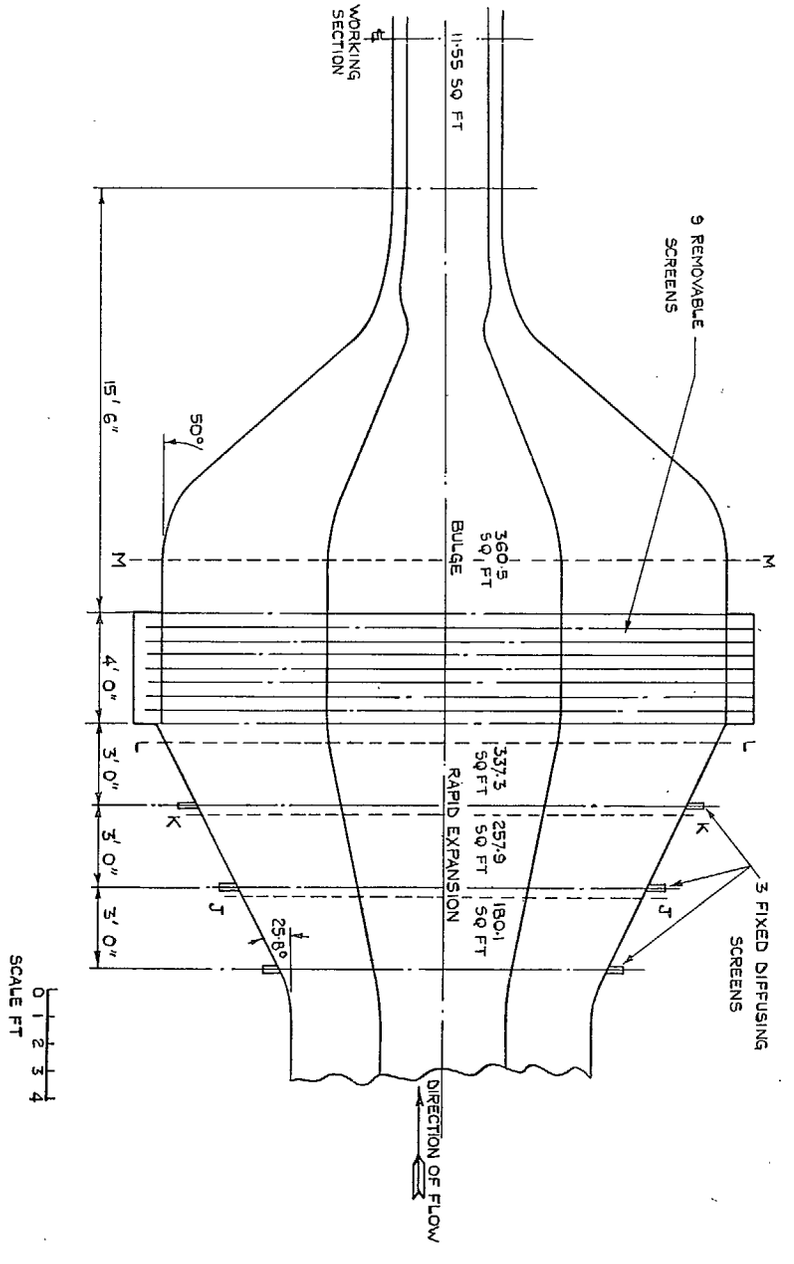

FIG. 21. Diagram showing positions of traverses.

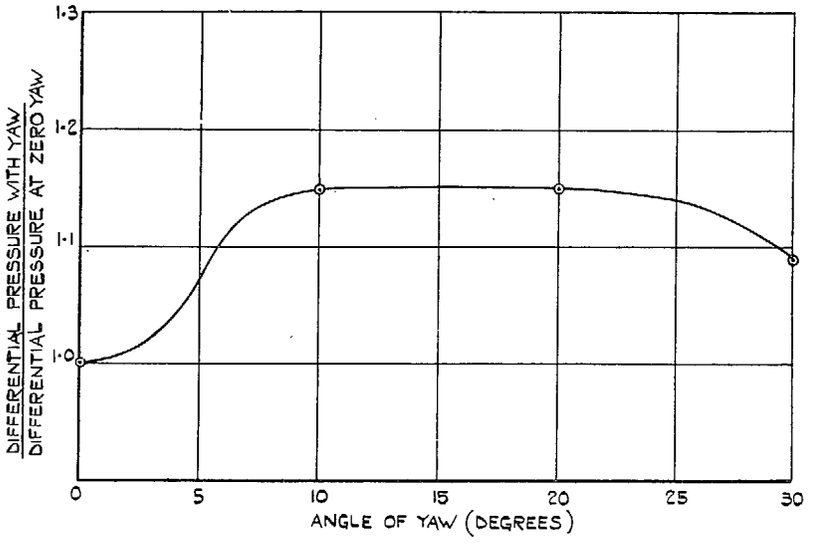

FIG. 19. Effect of yaw at 10 ft/sec.

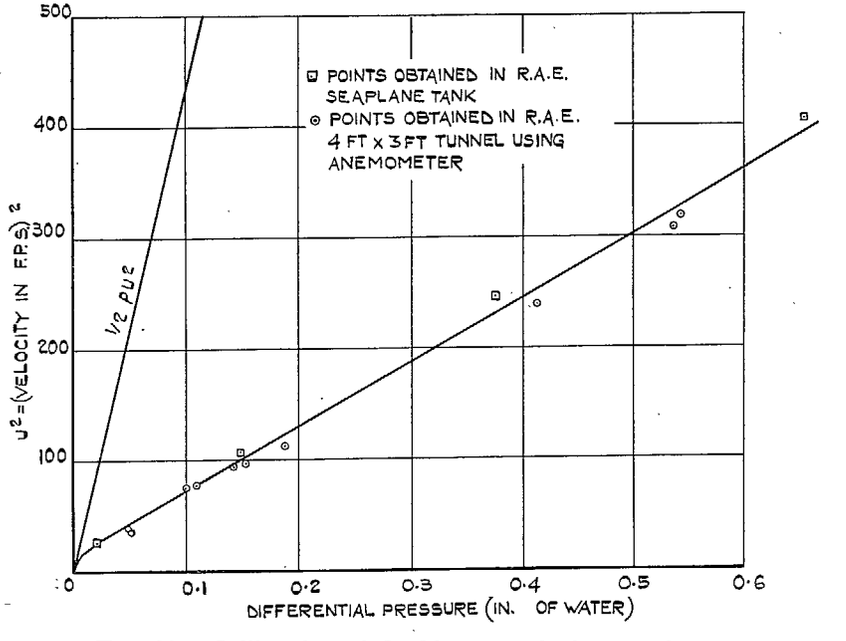

FIG. 20. Calibration of double venturi pitot static at 0 deg yaw.

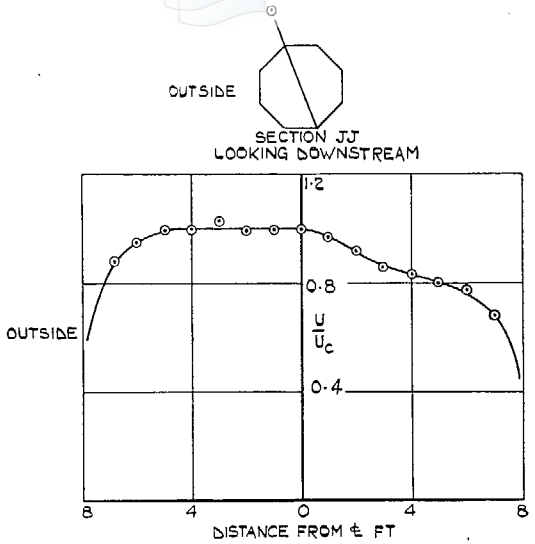

FIG. 22a. Velocity distribution between first and second fixed screens.

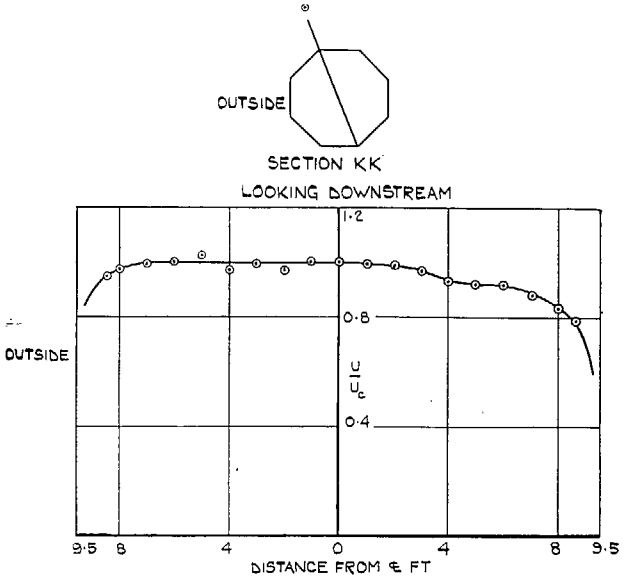

FIG. 22b. Velocity distribution between second and third fixed screens.

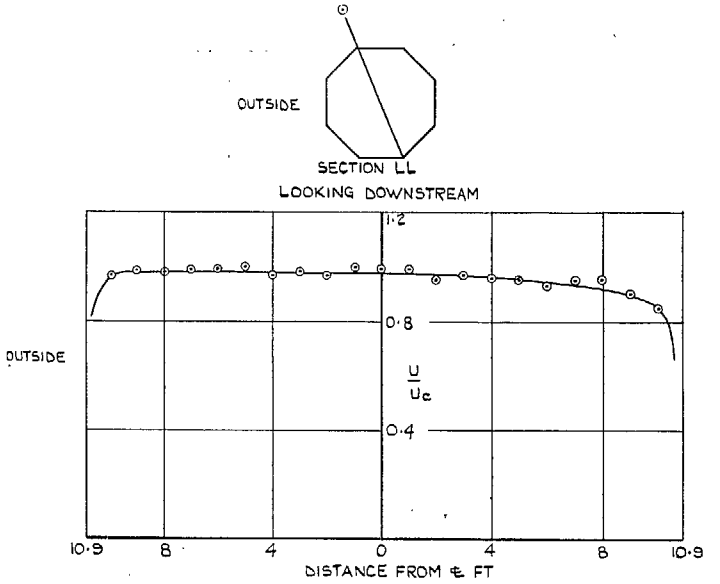

FIG. 22c. Velocity distribution between third fixed screen and first movable screen.

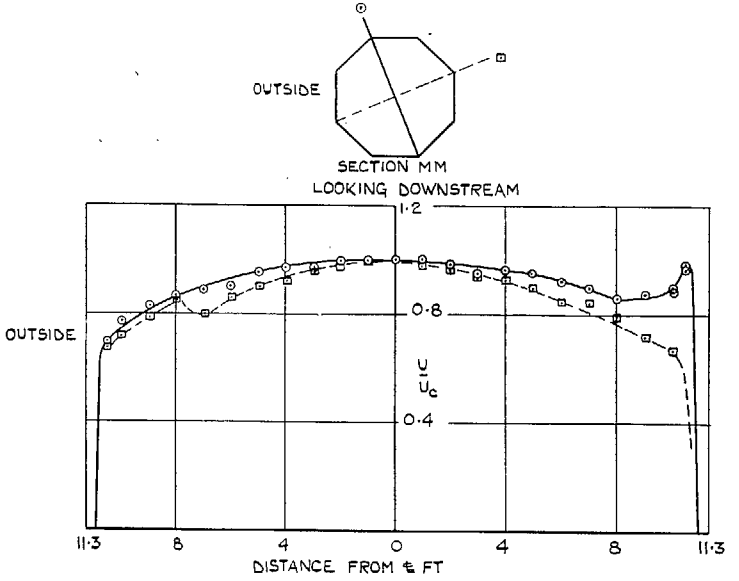

FIG. 22d. Velocity distribution downstream of all screens.

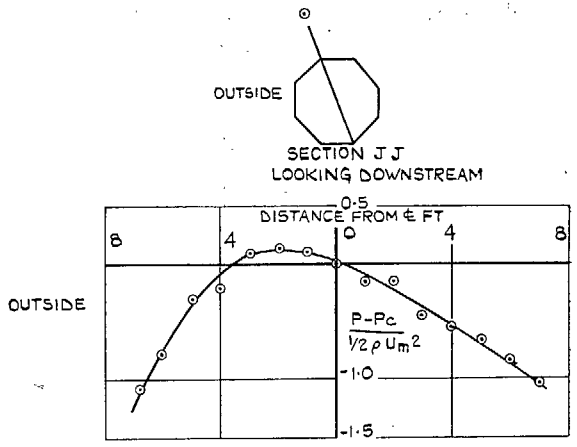

FIG. 23a. Total head between first and second fixed screens.

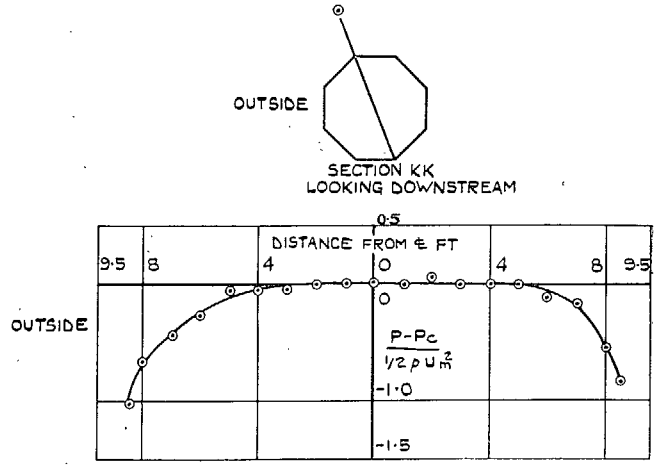

FIG. 23b. Total head between second and third fixed screens.

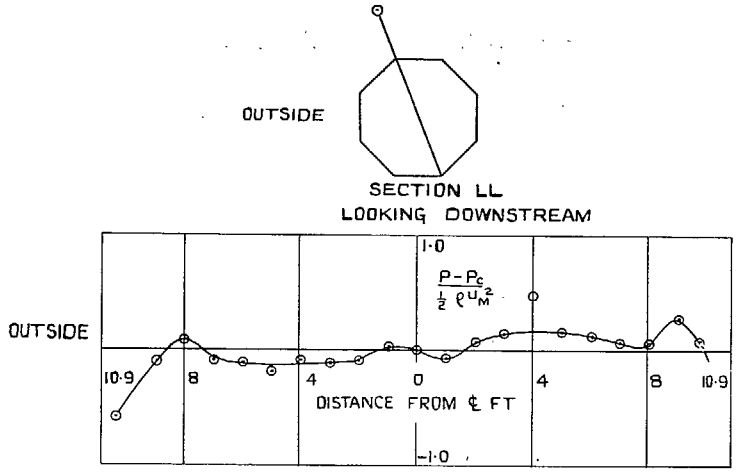

FIG. 23c. Total head between third fixed screen and first movable screen

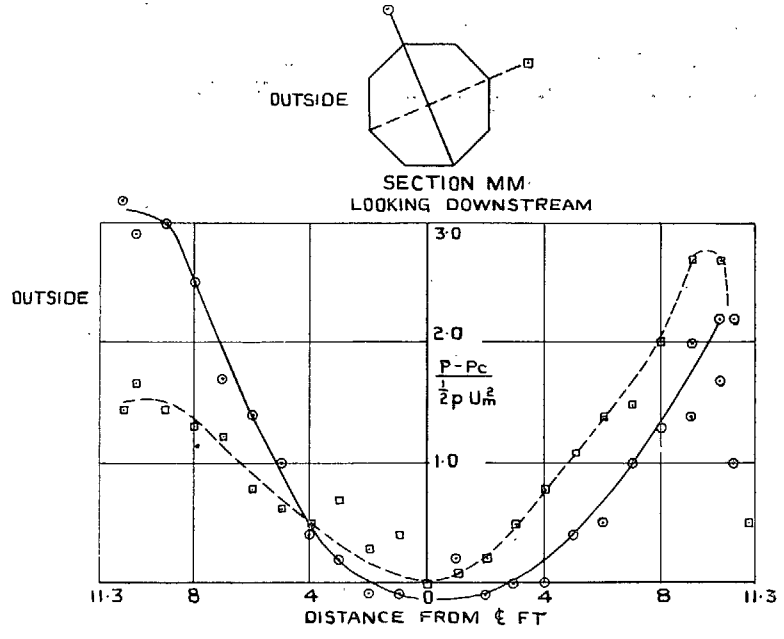

FIG. 23d. Total head downstream of all screens.

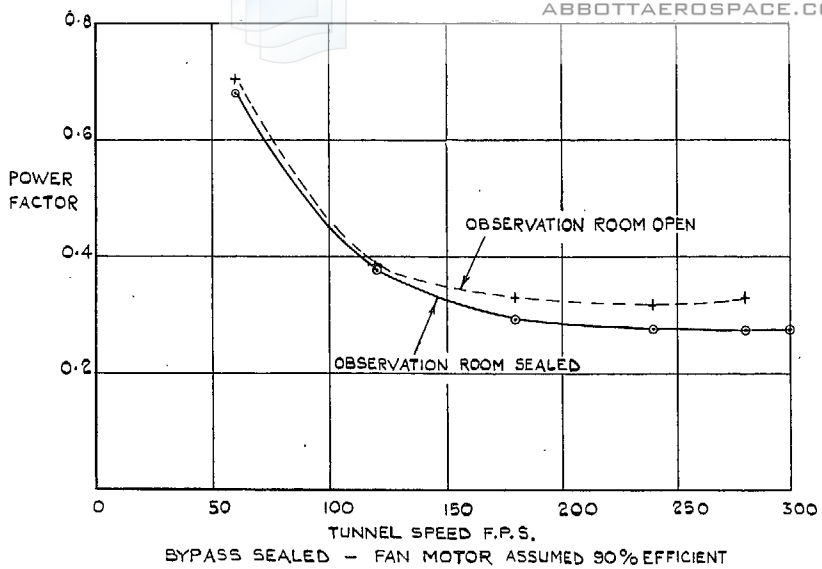

FIG. 24. Tunnel power factor.

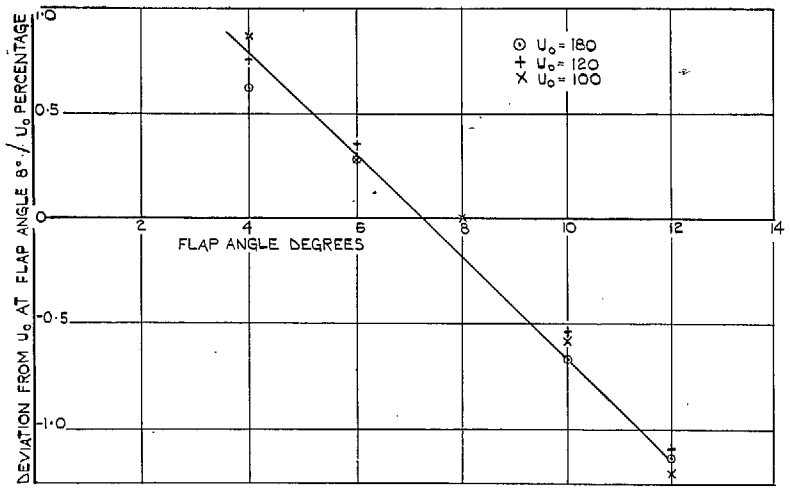

FIG. 26. Speed range covered by flap movement.

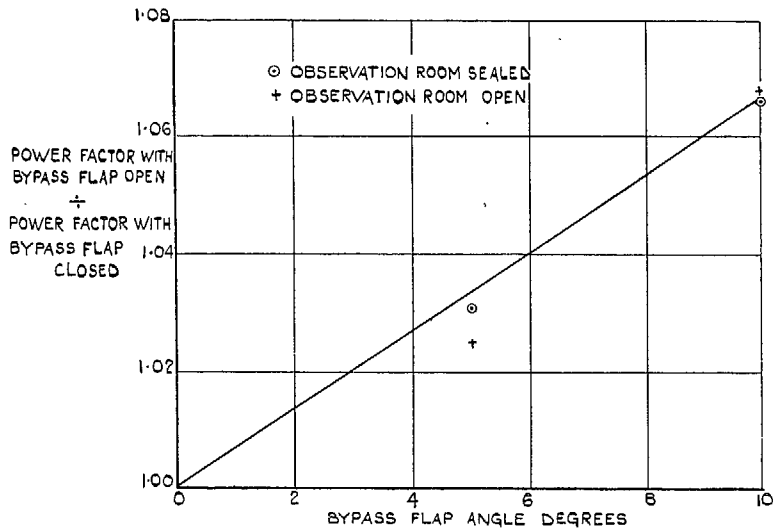

FIG. 25. Effect of by-pass flow on power factor.

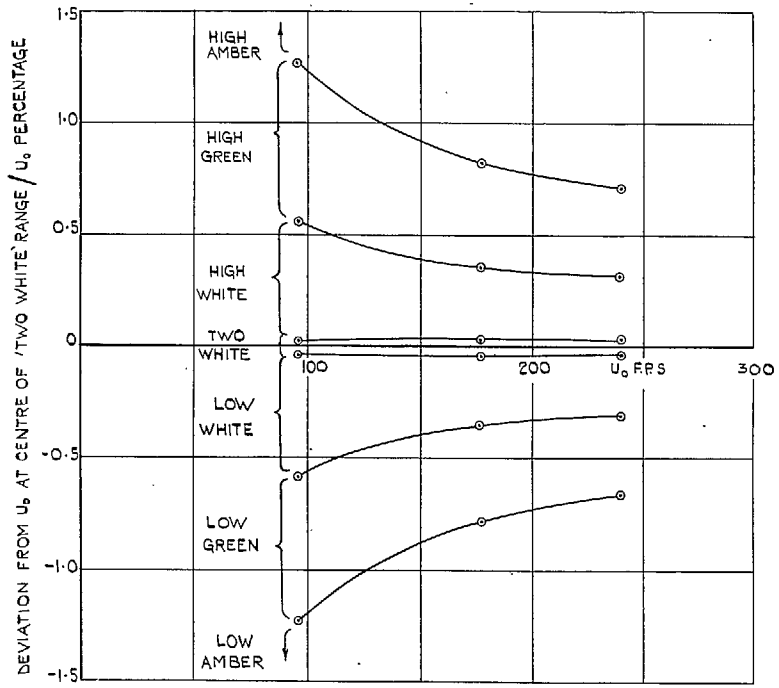

FIG. 27. Speed range of auto-manometer signal lights.

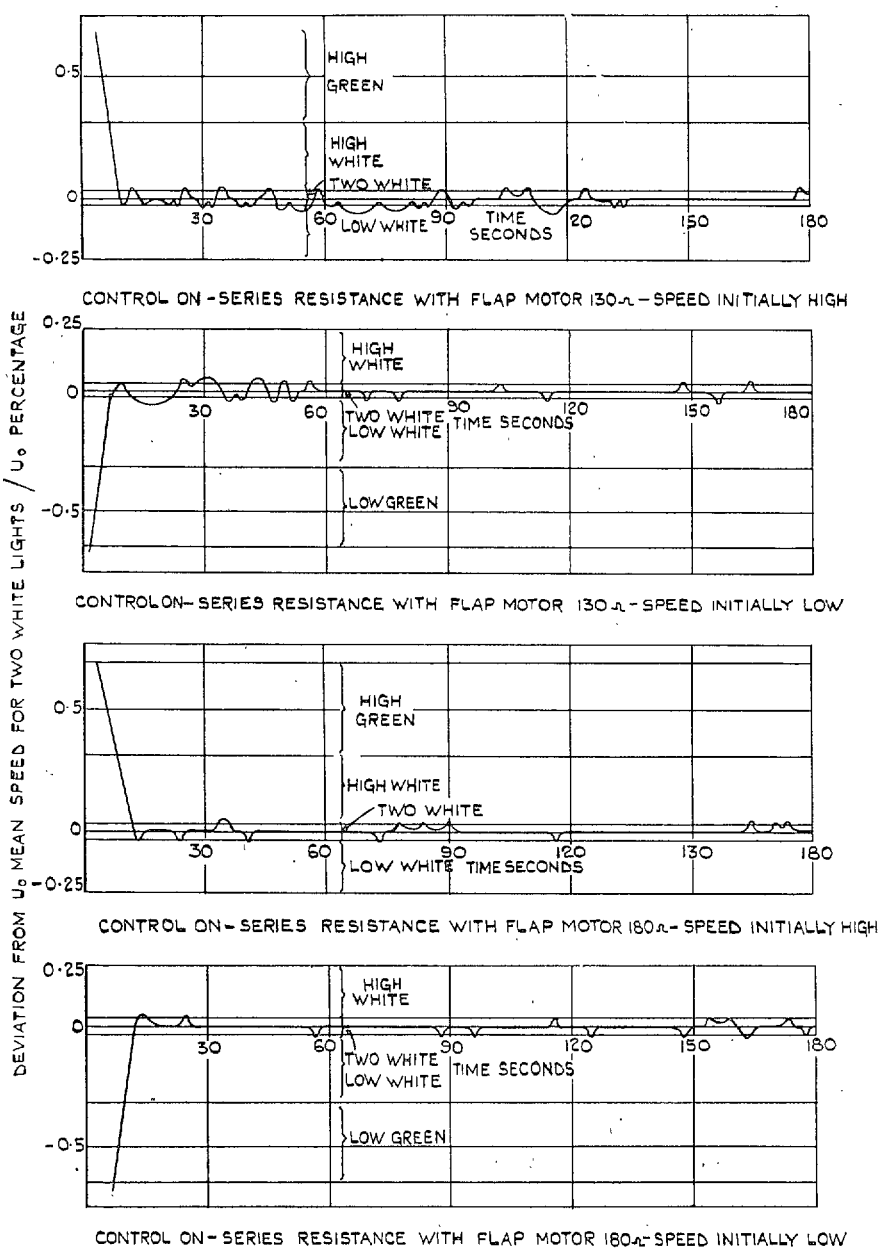

FIG. 28. Operation of automatic speed-control. $U_0 = 260$ ft/sec.

(52210) Wt. 15/680 K9 4/53 Hw. PRINTED IN GREAT BRITAIN

R. & M. No. 2690
(10,695 11,410)
A.R.C. Technical Report

Publications of the Aeronautical Research Council

ANNUAL TECHNICAL REPORTS OF THE AERONAUTICAL RESEARCH COUNCIL (BOUND VOLUMES)

1936 Vol. I. Aerodynamics General, Performance, Airscrews, Flutter and Spinning. 40*s.* (40*s.* 9*d.*)
Vol. II. Stability and Control, Structures, Seaplanes, Engines, etc. 50*s.* (50*s.* 10*d.*)

1937 Vol. I. Aerodynamics General, Performance, Airscrews, Flutter and Spinning. 40*s.* (40*s.* 10*d.*)
Vol. II. Stability and Control, Structures, Seaplanes, Engines, etc. 60*s.* (61*s.*)

1938 Vol. I. Aerodynamics General, Performance, Airscrews. 50*s.* (51*s.*)
Vol. II. Stability and Control, Flutter, Structures, Seaplanes, Wind Tunnels, Materials. 30*s.* (30*s.* 9*d.*)

1939 Vol. I. Aerodynamics General, Performance, Airscrews, Engines. 50*s.* (50*s.* 11*d.*)
Vol. II. Stability and Control, Flutter and Vibration, Instruments, Structures, Seaplanes, etc. 63*s.* (64*s.* 2*d.*)

1940 Aero and Hydrodynamics, Aerofoils, Airscrews, Engines, Flutter, Icing, Stability and Control, Structures, and a miscellaneous section. 50*s.* (51*s.*)

1941 Aero and Hydrodynamics, Aerofoils, Airscrews, Engines, Flutter, Stability and Control, Structures. 63*s.* (64*s.* 2*d.*)

1942 Vol. I. Aero and Hydrodynamics, Aerofoils, Airscrews, Engines. 75*s.* (76*s.* 3*d.*)
Vol. II. Noise, Parachutes, Stability and Control, Structures, Vibration, Wind Tunnels 47*s.* 6*d.* (48*s.* 5*d.*)

1943 Vol. I. (*In the press.*)
Vol. II. (*In the press.*)

ANNUAL REPORTS OF THE AERONAUTICAL RESEARCH COUNCIL—

1933–34	1*s.* 6*d.* (1*s.* 8*d.*)	1937	2*s.* (2*s.* 2*d.*)
1934–35	1*s.* 6*d.* (1*s.* 8*d.*)	1938	1*s.* 6*d.* (1*s.* 8*d.*)
April 1, 1935 to Dec. 31, 1936.	4*s.* (4*s.* 4*d.*)	1939–48	3*s.* (3*s.* 2*d.*)

INDEX TO ALL REPORTS AND MEMORANDA PUBLISHED IN THE ANNUAL TECHNICAL REPORTS, AND SEPARATELY—

April, 1950 - - - - R. & M. No. 2600. 2*s.* 6*d.* (2*s.* 7½*d.*)

AUTHOR INDEX TO ALL REPORTS AND MEMORANDA OF THE AERONAUTICAL RESEARCH COUNCIL—

1909–1949. R. & M. No. 2570. 15*s.* (15*s.* 3*d.*)

INDEXES TO THE TECHNICAL REPORTS OF THE AERONAUTICAL RESEARCH COUNCIL—

December 1, 1936 — June 30, 1939.	R. & M. No. 1850.	1*s.* 3*d.* (1*s.* 4½*d.*)
July 1, 1939 — June 30, 1945.	R. & M. No. 1950.	1*s.* (1*s.* 1½*d.*)
July 1, 1945 — June 30, 1946.	R. & M. No. 2050.	1*s.* (1*s.* 1½*d.*)
July 1, 1946 — December 31, 1946.	R. & M. No. 2150.	1*s.* 3*d.* (1*s.* 4½*d.*)
January 1, 1947 — June 30, 1947.	R. & M. No. 2250.	1*s.* 3*d* (1*s.* 4½*d.*)
July, 1951.	R. & M. No. 2350.	1*s.* 9*d.* (1*s.* 10½*d.*)

Prices in brackets include postage.

Obtainable from

HER MAJESTY'S STATIONERY OFFICE

York House, Kingsway, London, W.C.2; 423 Oxford Street, London, W.1 (Post Orders: P.O. Box 569, London, S.E.1); 13a Castle Street, Edinburgh 2; 39, King Street, Manchester, 2; 2 Edmund Street, Birmingham 3; 1 St. Andrew's Crescent, Cardiff; Tower Lane, Bristol 1; 80 Chichester Street, Belfast, or through any bookseller

S.O. Code No. 23–2690